American Journal of Physical Anthropology

Copy of e-mail Notification

American Journal of Physical Anthropology Published by John Wiley & Sons, Inc.

Dear Author,

Your article page proof for American Journal of Physical Anthropology is ready for your final content correction within our rapid production workflow. The PDF file found at the URL given below is generated to provide you with a proof of the content of your manuscript. Once you have submitted your corrections, the production office will proceed with the publication of your article.

John Wiley & Sons has made this article available to you online for faster, more efficient editing. Please follow the instructions below and you will be able to access a PDF version of your article as well as relevant accompanying paperwork.

First, make sure you have a copy of Adobe Acrobat Reader software to read these files. This is free software and is available for user downloading at (http://www.adobe.com/products/acrobat/readstep.html).

Open your web browser, and enter the following web address:
http://115.111.50.156/jw/retrieval.aspx?pwd=b8fe9ae8c404

You will be prompted to log in, and asked for a password. Your login name will be your email address, and your password will be b8fe9ae8c404

Example:
Login: your e-mail address
Password: b8fe9ae8c404

The site contains one file, containing:

--Author Instructions Checklist
--Instructions on the Annotation of PDF Files
--Reprint Order Information
--Color Reproduction Charge Form
--A copy of your page proofs for your article

In order to speed the proofing process, we strongly encourage authors to correct proofs by annotating PDF files.

Please see the Instructions on the Annotation of PDF files included with your page proofs. Please take care to answer all queries on the last page of the PDF proof; proofread any tables and equations carefully; and check that any Greek characters (especially "mu") have converted correctly. Please read your figure legends carefully.

# American Journal of Physical Anthropology

Copy of e-mail Notification

Within 1 to 2 business days please return your annotated PDF with corrections and comments and any relevant forms to: Production Editor, AJPA E-mail: jrnlprodajpa@cadmus.com

Technical problems? If you experience technical problems downloading your file or any other problem with the website listed above, please contact Balaji/Sam/Ganesh (e-mail: Wiley.CS@cenveo.com, phone: +91 (44) 4205-8810 (ext.308)). Be sure to include your article number.

Questions regarding your article? Please don't hesitate to contact me with any questions about the article itself, or if you have trouble interpreting any of the questions listed at the end of your file. REMEMBER TO INCLUDE YOUR ARTICLE NO. (23061) WITH ALL CORRESPONDENCE. This will help us address your query most efficiently.

As this e-proofing system was designed to make the publishing process easier for everyone, we welcome any and all feedback. Thanks for participating in our e-proofing system!

This e-proof is to be used only for the purpose of returning corrections to the publisher.

Sincerely,
Production Editor, AJPA
Email: jrnlprodajpa@cadmus.com

WILEY
*Publishers Since 1807*

111 RIVER STREET, HOBOKEN, NJ 07030

*****IMMEDIATE RESPONSE REQUIRED*****

Your article will be published online via Wiley's EarlyView® service (wileyonlinelibrary.com) shortly after receipt of corrections. EarlyView® is Wiley's online publication of individual articles in full text HTML and/or pdf format before release of the compiled print issue of the journal. Articles posted online in EarlyView® are peer-reviewed, copyedited, author corrected, and fully citable via the article DOI (for further information, visit www.doi.org). EarlyView® means you benefit from the best of two worlds--fast online availability as well as traditional, issue-based archiving.

Please follow these instructions to avoid delay of publication.

☐ **READ PROOFS CAREFULLY**

- This will be your only chance to review these proofs. **Please note that once your corrected article is posted online, it is considered legally published, and cannot be removed from the Web site for further corrections.**
- Please note that the volume and page numbers shown on the proofs are for position only.

☐ **ANSWER ALL QUERIES ON PROOFS** (Queries for you to answer are attached as the last page of your proof.)

- Please annotate all corrections and remember to respond to all author queries at the back of your page proofs.

☐ **CHECK FIGURES AND TABLES CAREFULLY**

- Check size, numbering, and orientation of figures.
- All images in the PDF are downsampled (reduced to lower resolution and file size) to facilitate Internet delivery. These images will appear at higher resolution and sharpness in the printed article.
- Review figure legends to ensure that they are complete.
- Check all tables. Review layout, title, and footnotes.

**RETURN** ☐ **PROOFS**

☐ **COLOR FORMS**

**RETURN WITHIN TWO BUSINESS DAYS OF RECEIPT**

**QUESTIONS?** Production Editor, AJPA
E-mail: jrnlprodajpa@cadmus.com
Refer to journal acronym and article production number

# USING e-ANNOTATION TOOLS FOR ELECTRONIC PROOF CORRECTION

Once you have Acrobat Reader open on your computer, click on the Comment tab at the right of the toolbar:

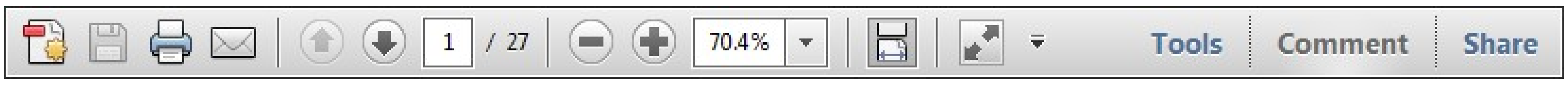

This will open up a panel down the right side of the document. The majority of tools you will use for annotating your proof will be in the Annotations section, pictured opposite. We've picked out some of these tools below:

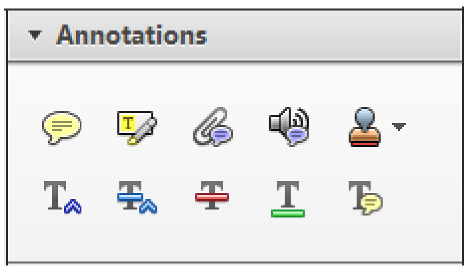

### 1. Replace (Ins) Tool – for replacing text.

Strikes a line through text and opens up a text box where replacement text can be entered.

**How to use it**

- Highlight a word or sentence.
- Click on the Replace (Ins) icon in the Annotations section.
- Type the replacement text into the blue box that appears.

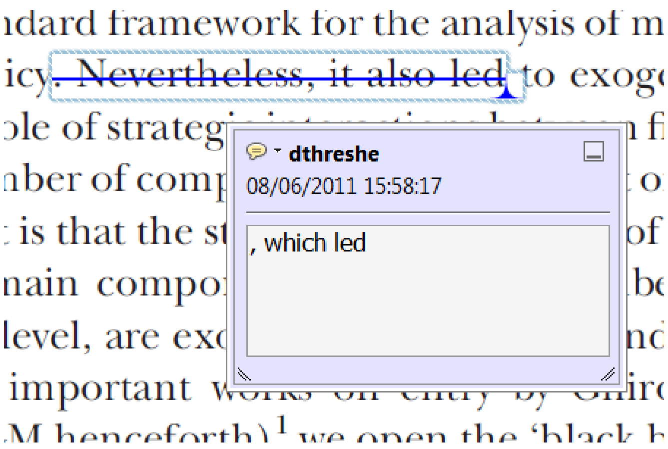

ıdard framework for the analysis of m
icy~~. Nevertheless, it also led~~ to exog

dthreshe
08/06/2011 15:58:17
, which led

### 2. Strikethrough (Del) Tool – for deleting text.

Strikes a red line through text that is to be deleted.

**How to use it**

- Highlight a word or sentence.
- Click on the Strikethrough (Del) icon in the Annotations section.

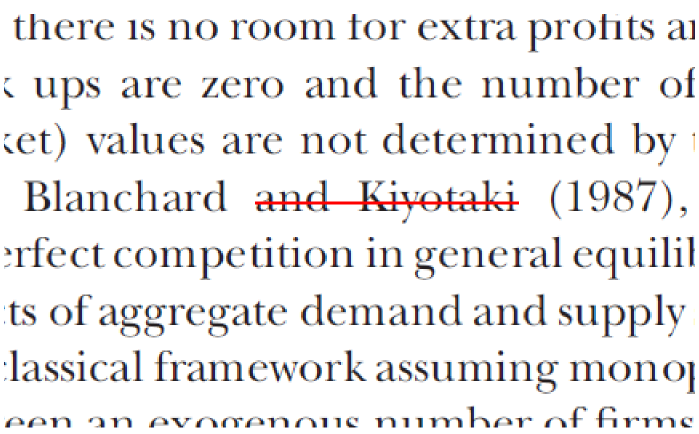

there is no room for extra profits a
ups are zero and the number of
ket) values are not determined by
Blanchard ~~and Kiyotaki~~ (1987),
erfect competition in general equili
ts of aggregate demand and supply
lassical framework assuming mono

### 3. Add note to text Tool – for highlighting a section to be changed to bold or italic.

Highlights text in yellow and opens up a text box where comments can be entered.

**How to use it**

- Highlight the relevant section of text.
- Click on the Add note to text icon in the Annotations section.
- Type instruction on what should be changed regarding the text into the yellow box that appears.

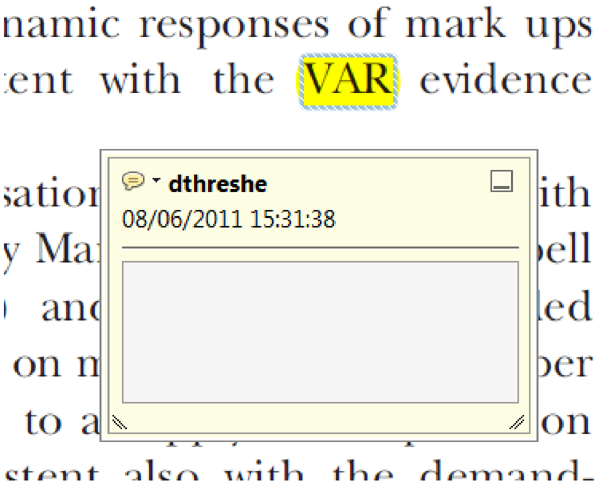

namic responses of mark ups
ent with the VAR evidence

dthreshe
08/06/2011 15:31:38

### 4. Add sticky note Tool – for making notes at specific points in the text.

Marks a point in the proof where a comment needs to be highlighted.

**How to use it**

- Click on the Add sticky note icon in the Annotations section.
- Click at the point in the proof where the comment should be inserted.
- Type the comment into the yellow box that appears.

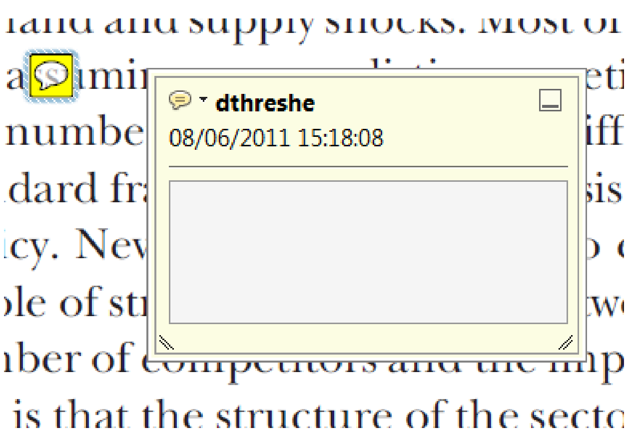

dthreshe
08/06/2011 15:18:08

### 5. Attach File Tool – for inserting large amounts of text or replacement figures.

Inserts an icon linking to the attached file in the appropriate pace in the text.

**How to use it**

- Click on the Attach File icon in the Annotations section.
- Click on the proof to where you'd like the attached file to be linked.
- Select the file to be attached from your computer or network.
- Select the colour and type of icon that will appear in the proof. Click OK.

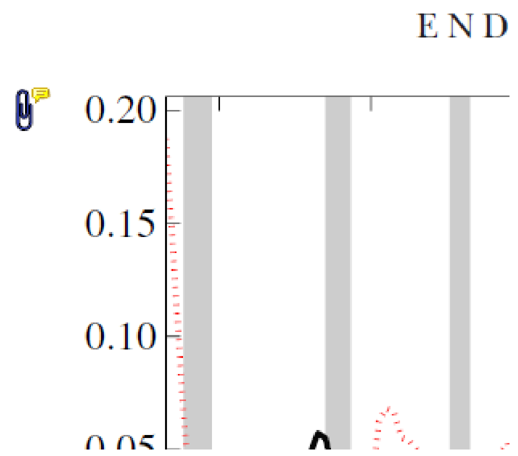

### 6. Drawing Markups Tools – for drawing shapes, lines and freeform annotations on proofs and commenting on these marks.

Allows shapes, lines and freeform annotations to be drawn on proofs and for comment to be made on these marks.

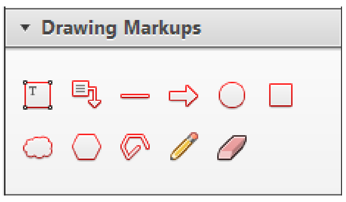

**How to use it**

- Click on one of the shapes in the Drawing Markups section.
- Click on the proof at the relevant point and draw the selected shape with the cursor.
- To add a comment to the drawn shape, move the cursor over the shape until an arrowhead appears.
- Double click on the shape and type any text in the red box that appears.

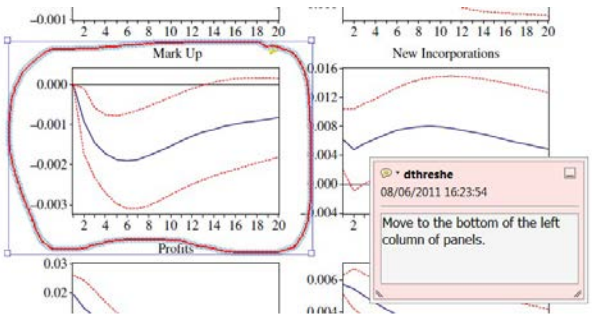

dthreshe
08/06/2011 16:23:54
Move to the bottom of the left column of panels.

Received: 16 November 2015 | Revised: 14 June 2016 | Accepted: 24 July 2016

DOI 10.1002/ajpa.23061

RESEARCH ARTICLE

WILEY American Journal of PHYSICAL ANTHROPOLOGY The Official Journal of the American Association of Physical Anthropologists

# Trabecular architecture in the thumb of Pan and Homo: implications for investigating hand use, loading, and hand preference in the fossil record

AQ9 **Nicholas B. Stephens**[1] | **Tracy L. Kivell**[1,2] | **Thomas Gross**[3] | **Dieter H. Pahr**[3] | **Richard A. Lazenby**[4] | **Jean-Jacques Hublin**[1] | **Israel Hershkovitz**[5] | **Matthew M. Skinner**[1,2]

[1]Department of Human Evolution, Max Planck Institute for Evolutionary Anthropology, Deutscher Platz 6, Leipzig 04103, Germany

[2]School of Anthropology and Conservation, Skeletal Biology Research Centre, University of Kent, Canterbury CT2 7NR, United Kingdom

[3]Institute of Lightweight Design and Structural Biomechanics, Vienna University of Technology, A-1060 Vienna, Getreidemarkt 9/BE, Vienna, Austria

[4]Department of Anthropology, University of Northern British Columbia, 3333 University Way, Prince George, BC, Canada V2N 4Z9

[5]Department of Anatomy and Anthropology, Sackler Faculty of Medicine, Tel-Aviv University, Tel-Aviv, Israel

**Correspondence**

Nicholas B. Stephens, Department of Human Evolution, Max Planck Institute for Evolutionary Anthropology, Deutscher Platz 6, Leipzig 04103, Germany.

Email: nick_stephens@eva.mpg.de

## Abstract

**Objectives:** Humans display an 85–95% cross-cultural right-hand bias in skilled tasks, which is considered a derived behavior because such a high frequency is not reported in wild non-human primates. Handedness is generally considered to be an evolutionary byproduct of selection for manual dexterity and augmented visuo-cognitive capabilities within the context of complex stone tool manufacture/use. Testing this hypothesis requires an understanding of when appreciable levels of right dominant behavior entered the fossil record. Because bone remodels *in vivo*, skeletal asymmetries are thought to reflect greater mechanical loading on the dominant side, but incomplete preservation of external morphology and ambiguities about past loading environments complicate interpretations. We test if internal trabecular bone is capable of providing additional information by analyzing the thumb of Homo sapiens and Pan.

**Materials and methods:** We assess trabecular structure at the distal head and proximal base of paired (left/right) first metacarpals using micro-CT scans of Homo sapiens ($n = 14$) and Pan ($n = 9$). Throughout each epiphysis we quantify average and local bone volume fraction (BV/TV), degree of anisotropy (DA), and elastic modulus ($E$) to address bone volume patterning and directional asymmetry.

**Results:** We find a right directional asymmetry in H. sapiens consistent with population-level handedness, but also report a left directional asymmetry in Pan that may be the result of postural and/or locomotor loading.

**Conclusion:** We conclude that trabecular bone is capable of detecting right/left directional asymmetry, but suggest coupling studies of internal structure with analyses of other skeletal elements and cortical bone prior to applications in the fossil record.

KEYWORDS

biomechanics, hand evolution, hominin behavior, microstructure, skeletal asymmetry

## 1 | THE EVOLUTION OF HAND PREFERENCE AND HANDEDNESS

AQ1

Handedness is a lateralized behavior that refers to the consistent, preferential use of either the right- or left-hand across skilled manipulative tasks (Marchant & McGrew, 2013; McGrew & Marchant, 1997). A right-hand bias is frequently reported in humans to be between ~85% and 95% cross-culturally, and thus is considered a population-level behavior (Faurie, Schiefenhovel, Le Bomin, Billiard, & Raymond, 2005). Being that many functional asymmetries are now recognized across vertebrates, (Cowell, Waters, & Denenberg, 1997; Frühholz et al., 2015; Indersmitten & Gur, 2003; Lewis, Phinney, Brefczynski-Lewis, &

DeYoe, 2006; Roth, Lora, & Heilman, 2002; Tate, Fischer, Leigh, & Kendrick, 2006; Weiss, Ghazanfar, Miller, & Hauser, 2002), we understand such biases to be widespread and ancient (Andrew & Rogers, 2002). While the genetic determinants of handedness remain elusive, genome-wide association studies support heritability for hand preference in humans (Armour, Davison, & McManus, 2014; McManus, Davison, & Armour, 2013) and chimpanzees (Pan troglodytes) (Hopkins, Reamer, Mareno, & Schapiro, 2015).

In contrast to humans, observational studies of individual hand preference in other primates have determined that variation in posture (Braccini, Lambeth, Schapiro, & Fitch, 2010; Dodson, Stafford, Forsythe, Seltzer, & Ward, 1992; Olson, Ellis, & Nadler, 1990), task complexity (Bardo, Pouydebat, & Meunier, 2015; Byrne & Byrne, 1991; Hopkins, 1995), and terrestriality (Marchant & McGrew, 2007; Miller & Paciulli, 2002) all have an impact on the strength of hand preference. While chimpanzees do demonstrate a consistent preference across tasks at an individual level (Marchant & McGrew, 2013), a group/species level side-bias remains unobserved in the wild (e.g., Boesch, 1991; McGrew & Marchant, 1992) and only weakly present in captive populations (∼65% right directional asymmetry) (e.g., Hopkins et al., 2011; Tabiowo & Forrester, 2013). Although the latter point speaks to a potential capacity (Hopkins, 2013), confounding factors in captive populations—such as task transmission through human observation (Marchant & McGrew, 2013)—suggest that species level right-hand preference evolved following the panin-hominin split (Corballis, 2003), and potentially only within Homo (Lozano, Mosquera, Bermúdez de Castro, Arsuaga, & Carbonell, 2009; Uomini, 2011).

In response to these observations, many have proposed that the species-level right directional asymmetry in humans coevolved with (1) an intensified reliance upon increasingly complex stone tool manufacture/use from at least ∼2.6 Ma (Semaw et al., 2003; Steele, 2004; Steele & Uomini, 2005) to possibly ∼3.3 Ma (Harmand et al., 2015), and with (2) selection for a highly dexterous hand working in conjunction with an augmented suite of visuo-cognitive functional asymmetries (Cantalupo, Freeman, Rodes, & Hopkins, 2008; Fitch & Braccini, 2013; Hopkins, 2013; Meguerditchian, Vauclair, & Hopkins, 2010; Steele & Uomini, 2005; Stout & Chaminade, 2012; Stout, Toth, Schick, & Chaminade, 2008). Testing these proposed cause and effect relationships in this coevolution model hinges largely on the timing of when hand preference became fixed in past populations (Steele, 2004; Ubelaker & Zarenko, 2012; Uomini, 2009). Archaeological techniques for addressing this question rely on right/left directional asymmetries in the production of rock-art stencils of the hand (Faurie & Raymond, 2004), or signs of striking preference during stone flake tool production (Rugg & Mullane, 2001; Toth, 1985; but see Ruck, Broadfield, & Brown, 2015) and use (Phillipson, 1997). The value of such analyses is apparent, but their interpretive power is limited by time-averaging, the sparse availability of examples at the onset of the archaeological record, and their disassociation from a specific individual/group/species (Cashmore, Uomini, & Chapelain, 2008). Other techniques, such as skeletal analysis, suffer from missing and incomplete remains, but provide information on individual and group-level preference by detecting consistent morphological departures from normal right/left symmetry (Auerbach & Ruff, 2006; Van Valen, 1962) that are beyond the random fluctuating asymmetries resulting from environmental stress (Palmer, 1994). Such directional bias has been observed in striations accruing from meat cut between clenched incisors (Bermúdez de Castro, Bromage, & Jalvo, 1988; Frayer et al., 2012; Lozano et al., 2009) and asymmetrical bone remodeling in response to frequent loading of the humeri on the dominant side (Volpato et al., 2012).

## 1.1 | Bone functional adaptation, loading, and handedness

Bone's tendency to remodel in response to the mechanical environment—broadly referred to as bone functional adaptation (Currey, 2003)—is best explained by the mechanostat model (Frost, 1987), which holds that bone mass is regulated by the continual removal and renewal of strain-damaged bone. Biomechanically, morphological variation in both cortical (Bass et al., 2002; Shaw, 2011; Stock, 2006) and trabecular bone (Lambers et al., 2013; Morgan et al., 2015; Schulte et al., 2013) strongly correlates with the loading environment (Christen et al., 2014). Within tubular bones, the most frequently observed correlation is found in variation of cross-sectional geometry at the mid-shaft (Marchi, 2005; Ruff, Holt, & Trinkaus, 2006; Ruff & Jones, 1981), which is thought to remodel in a way that confers greater resistance to bending and torsion (but see Demes et al., 1998; Wallace, Judex, & Demes, 2015; and below). Similarly, *in vivo* studies analyzing homologous volumes of interest (VOI) of trabeculae at the epiphysis (e.g., Barak, Lieberman, & Hublin, 2011; Mittra, Rubin, & Qin, 2005; Pontzer et al., 2006) demonstrate that differences in loading regimes results in changes to the orientation, thickness, connectivity, spacing, and overall distribution of this structure (e.g., Lambers et al., 2013; Reznikov, Chase, Brumfeld, Shahar, & Weiner, 2015). This variation in trabecular structure allows joint reaction forces to be efficiently transferred away from the articular surface and into the cortices (Currey, 2003; Keaveny, Morgan, Niebur, & Yeh, 2001; Lieberman, Devlin, & Pearson, 2001; Rafferty & Ruff, 1994).

Following this model, biomechanical studies focusing on variation in osseous tissue have advanced our understanding of the interrelationships among habitual behavior, locomotion, and loading environments for extant (Fajardo & Müller, 2001; Marchi, 2005; Ryan & Ketcham, 2002b; Ryan & Krovitz, 2006; Ryan & van Rietbergen, 2005; Ryan & Walker, 2010; Stock & Pfeiffer, 2001) and extinct primates (Barak et al., 2013; Ryan & Ketcham, 2002a; Trinkaus, Churchill, & Ruff, 1994). Studies applying this perspective to questions of hand preference frequently report a right directional asymmetry in mechanical resistance of the upper limbs (Barros & Soligo, 2013; Churchill & Formicola, 1997; Macintosh, Pinhasi, & Stock, 2014; Shaw, Hofmann, Petraglia, Stock, & Gottschall, 2012; Trinkaus et al., 1994;) and manual remains (Lazenby, 1998; Lazenby, Cooper, Angus, & Hallgrimsson, 2008; Mays, 2002; Roy, Ruff, & Plato, 1994; Singh, 1979) of past human populations that are commensurate with group/species-level right handedness. Such departures from right/left symmetry are thought to be the byproduct of frequent lateralized loading on the dominant side (Auerbach & Ruff, 2006; Kanchan, Mohan Kumar, Pradeep Kumar, & Yoganarasimha, 2008), which is supported by studies of uni-manual loading and self-reported hand preference in living athletes (Bass et al., 2002; Shaw, 2011).

Despite such results, the relationship between behavior and bone functional adaptation is not always straightforward. For example, variation in primate trabecular structure of different skeletal elements does not always correlate well with predicted loading based on locomotor behavior because of high intragroup variation or substantial overlap across different locomotor groups (e.g., Fajardo, Müller, Ketcham, & Colbert, 2007; Maga, Kappelman, Ryan, & Ketcham, 2006; Ryan & Shaw, 2012; Schilling et al., 2013). Furthermore, Shaw and Ryan (2012) found a consistent biomechanical signal in the cross-sectional geometry and trabecular architecture of the primate humerus but not in the femur. Such disagreement is consistent with Stock, Shirley, Sarringhaus, Davies, and Shaw (2013) who found that levels of right directional asymmetry in the paired humeri and second metacarpals differed across medieval, industrial, and hunter-gatherer populations. Of these groups, the hunter-gatherer group showed a much stronger right directional asymmetry in the humerus (83.6%) compared with second metacarpal (62.5%) (Stock et al., 2013). Although many of these studies do uphold an interpretation of some response to loading, it is clear that the mechanisms underlying bone functional adaptation are not fully understood (Currey, 2012) and that many other factors may contribute to changes in bone morphology.

Indeed, debate exists about the potential systemic impact on other areas of the skeleton when one bone/region is loaded (Cresswell, Goff, Nguyen, Lee, & Hernandez, 2016; Lieberman, 1996; Sample et al., 2008; Sugiyama, Price, & Lanyon, 2010; Wallace et al., 2010), and how bone remodeling changes in response to differences in age (Nikander et al., 2010; Pearson & Lieberman, 2004; Ruff et al., 2006), muscle (Robling, 2009) versus joint reaction loading (Judex & Carlson, 2009; Schipilow, Macdonald, Liphardt, Kan, & Boyd, 2013), force (Christen et al., 2014; Schulte et al., 2013), and even how these factors are balanced against the role of the bone in maintaining homeostasis (Currey, 2003). Beyond this, large scale genetic studies have identified independent loci for cortical and trabecular bone that are associated with higher risk of fracture (Paternoster et al., 2013; Yerges et al., 2010), which suggests certain fixed aspects to bone morphology that may be insensitive to loading. Similarly, investigations into the question of changes to bone density during hormonal osteoporotic intervention make it clear that the cellular response of the boney matrix is sensitive to physiological agents that might act to augment, nullify, or buffer the reaction to loading (Bahtiri et al., 2015; Xhae et al., 2015). Such complexities are highlighted in a recent study by Wallace et al. (2015) who used three cohorts of treadmill-exercised mice to clarify the relationship of peak-load and bone functional adaptation. In this study it was shown that although peak forces were greater in the forelimbs, only the hindlimbs of the exercised mice reflected meaningful cortical and trabecular skeletal adaptation, which, the authors suggested, could be explained by a non-uniform response of the cells responsible for bone growth and repair. In light of this, it is clear that new methods for detecting variances in bone morphology must be added to pre-existing ones to refine our understanding of the relationship between behavior, loading environment, function, and skeletal response (Cashmore et al., 2008; Lazenby, 2002; Steele, 2004).

With recent advances in computational power it is now feasible to analyze multiple VOIs (Su, Wallace, & Nakatsukasa, 2013) or the entire internal trabecular structure (Gross, Kivell, Skinner, Nguyen, & Pahr, 2014) to gain a greater understanding of how trabecular bone varies throughout an epiphysis or bone. The latter method allows the mapping of site-specific bone volume to total volume (BV/TV) and degree of anisotropy (DA) values onto a 3D tetrahedral mesh, thus facilitating the visual comparison of quantitative data. This is valuable because BV/TV is consistently shown to be the strongest predictor of fracture resistance (Keaveny et al., 2001; Maquer, Musy, Wandel, Gross, & Zysset, 2015; Stauber, Rapillard, van Lenthe, Zysset, & Müller, 2006), and understanding this site-specific distribution has already proven valuable in interpreting joint loading position related to locomotion and manual behavior in extant (Tsegai et al., 2013) and extinct (Skinner et al., 2015) primate hand bones. Furthermore, recent studies inspecting the localized nature of trabecular repair support the view that formation and remodeling sites correspond to areas of load (Christen et al., 2014; Cresswell et al., 2016; Schulte et al., 2013), which supports the idea of visualizing and describing this site-specific variation. If applied to bones of the hand, this method has strong potential relevance for reconstructing hominin manipulatory repertoires and the evolution of hand preference in the fossil record.

## 1.2 | Thumb loading and predictions

In humans many complex manual tasks utilize pinch, key, or power grips that are facilitated by a long thumb relative to the fingers (Ladd, Crisco, Hagert, Rose, & Weiss, 2014; Marzke, 1997; Napier, 1960; Susman, 1979). Such grips are important during stone tool manufacture and use (Marzke et al., 1998) and often involve forceful opposition provided by a derived set of thenar and pollical muscles that allows the tip of the thumb to flex while the base remains extended (e.g., when holding a needle) (Diogo, Richmond, & Wood, 2012; Marzke et al., 1999). Experimental studies have shown that during tool-related activities, loading of the thumb of the dominant hand is high (Rolian, Lieberman, & Zermeno, 2011; Williams, Gordon, & Richmond, 2012) compared with non-dominant thumb (Key & Dunmore, 2015). This differs from other great apes, such as Pan, that possess a short and comparatively weaker thumb (Marzke et al., 1999), and most often use less forceful pad-to-side precisions grips (Marzke & Wullstein, 1996; but see Marzke, Marchant, McGrew, & Reece, 2015) that are employed during, for example, nut-cracking (Boesch & Boesch, 1993) and ant-fishing (Marchant & McGrew, 2007). Because of such differences in anatomy and use between humans and other apes, the thumb remains the focus of multidisciplinary attempts to ascertain its biomechanical role (Cheema, Cheema, Tayyab, & Firoozbakhsh, 2006; Key & Lycett, 2011; Marzke et al., 1998) and evolutionary change over time (Diogo et al., 2012; Niewoehner, 2001, 2006; Niewoehner, Weaver, & Trinkaus, 1997; Shrewsbury, Marzke, Linscheid, & Reece, 2003; Smith, 2000; Tocheri

**TABLE 1** Average BV/TV, DA, and elastic modulus in the study sample

| | *Pan* pairs (*n* = 9) | | | | *Homo* pairs (*n* = 14) | | | | *Pan* (mean L&R) | | *Homo* (mean L&R) | | Between groups | |
|---|---|---|---|---|---|---|---|---|---|---|---|---|---|---|
| Variable | L | *SD* | R | *SD* | L | *SD* | R | *SD* | Mean | *SD* | Mean | *SD* | *U* | *p* Value |
| BV/TV head, % | 34.74 | (6.10) | 32.65 | (5.19) | 20.18 | (4.44) | 22.44 | (2.80) | 33.69 | (5.60) | 21.31 | (3.34) | 716 | <0.01 |
| BV/TV base, % | 27.12 | (3.84) | 26.83 | (4.53) | 16.86 | (3.33) | 18.96 | (2.66) | 26.74 | (4.06) | 17.91 | (2.78) | 714 | <0.01 |
| DA head | 1.04 | (0.11) | 1.00 | (0.01) | 1.28 | (0.17) | 1.29 | (0.17) | 1.02 | (0.06) | 1.29 | (0.11) | 88 | <0.01 |
| DA base | 1.22 | (0.25) | 1.14 | (0.17) | 1.30 | (0.15) | 1.34 | (0.18) | 1.18 | (0.20) | 1.32 | (0.15) | 76 | <0.01 |
| *E* head | 3.36 | (1.13) | 3.01 | (1.00) | 1.50 | (0.52) | 1.82 | (0.32) | 3.19 | (1.06) | 1.66 | (0.37) | 708 | <0.01 |
| *E* base | 2.40 | (0.72) | 2.28 | (0.819) | 1.17 | (0.37) | 1.43 | (0.31) | 2.34 | (0.75) | 1.30 | (0.31) | 708 | <0.01 |

Abbreviations (BV/TV = bone volume; DA = degree of anisotropy; *E* = elastic modulus in gigapascals; L&R = mean value of the mean (right and left sides) values; L = mean value of all left metacarpals; R = mean value of all right metacarpals; *SD* = standard deviation; *U* = Mann–Whitney *U* score; *p* = exact *p* value for Mann–Whitney *U* test).
Shaded boxes indicate left directional asymmetry.

et al., 2003; Tocheri, Orr, Jacofsky, & Marzke, 2008; Trinkaus & Villemeur, 1991; Villemeur, 1994; Vlček, 1975; see Almécija, Alba, & Moya-Sola, 2012; Almécija, Wallace, Judex, Alba, & Moya-Sola, 2015 for a view that certain features of the thumb are retained from Miocene apes).

To this end, we investigate trabecular architecture and directional asymmetry in the thumb of recent Homo sapiens and Pan to assess if such an analysis might be applied to questions of loading history and hand preference within the fossil record. Given the predictions of the mechanostat model (Currey, 2003; Frost, 1987), variation in loading of the thumb should be reflected in the first metacarpal (Mc1) because the pollical musculature passes along the base and head to attach at the phalanges (Brand & Hollister, 1993; Maki & Trinkaus, 2011; Marzke et al., 1998; Trinkaus & Villemeur, 1991), meaning this bone will be loaded both by joint reaction forces and muscular tension during flexion and opposition (Hu, Ren, Howard, & Zong, 2014; Kargov, Pylatiuk, Martin, Schulz, & Doderlein, 2004; Pataky, Slota, Latash, & Zatsiorsky, 2012). We predict that the H. sapiens first metacarpals will experience asymmetric loading reflecting group-level hand preference, while Pan should reflect no group bias. Although highly lateralized terrestrial galloping has been reported (Arcadi & Wallauer, 2011), the thumb is not loaded during terrestrial knuckle-walking (Matarazzo, 2013; Sarringhaus, MacLatchy, & Mitani, 2014; Wunderlich & Jungers, 2009). Potentially high and variable loading of the thumb is thought to occur during arboreal climbing, suspensory locomotion (Hunt, 1991, 1994; Marzke & Wullstein, 1996), and grips observed during feeding (Marzke et al., 2015), behaviors for which individuals can show a hand preference. However, the lack of directional asymmetry in a previous study of trabecular architecture of paired first, second, and fifth metacarpals of Pan troglodytes (Lazenby, Skinner, Hublin, & Boesch, 2011) suggest the same will be true for the first metacarpal in the present study.

Accordingly, we predict that (1) the BV/TV distribution and overall architectural trabecular pattern of the Mc1 will reflect variation in the

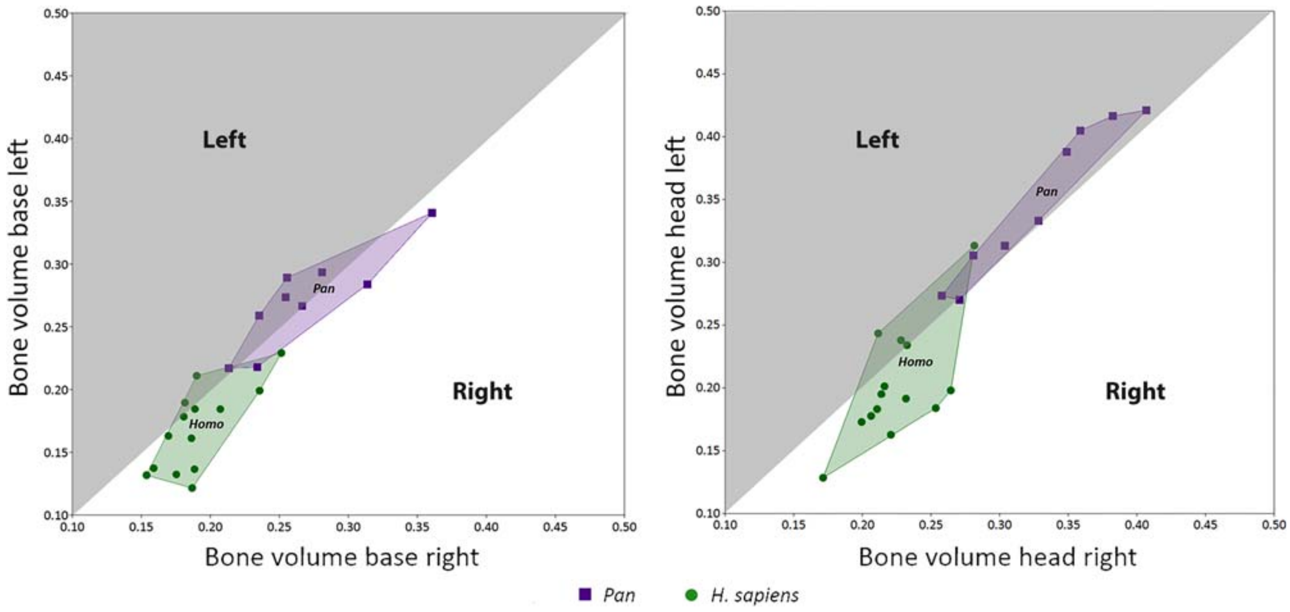

COLOR

**FIGURE 1** Bone volume of the first metacarpal base (left) and head (right) for both sides of each individual. Shaded area contains individuals demonstrating left directional asymmetry. *H. sapiens* (green dot) demonstrates a clear right directional asymmetry with relatively low BV/TV, while *Pan* (purple square) demonstrates a left directional asymmetry trend with relatively high BV/TV

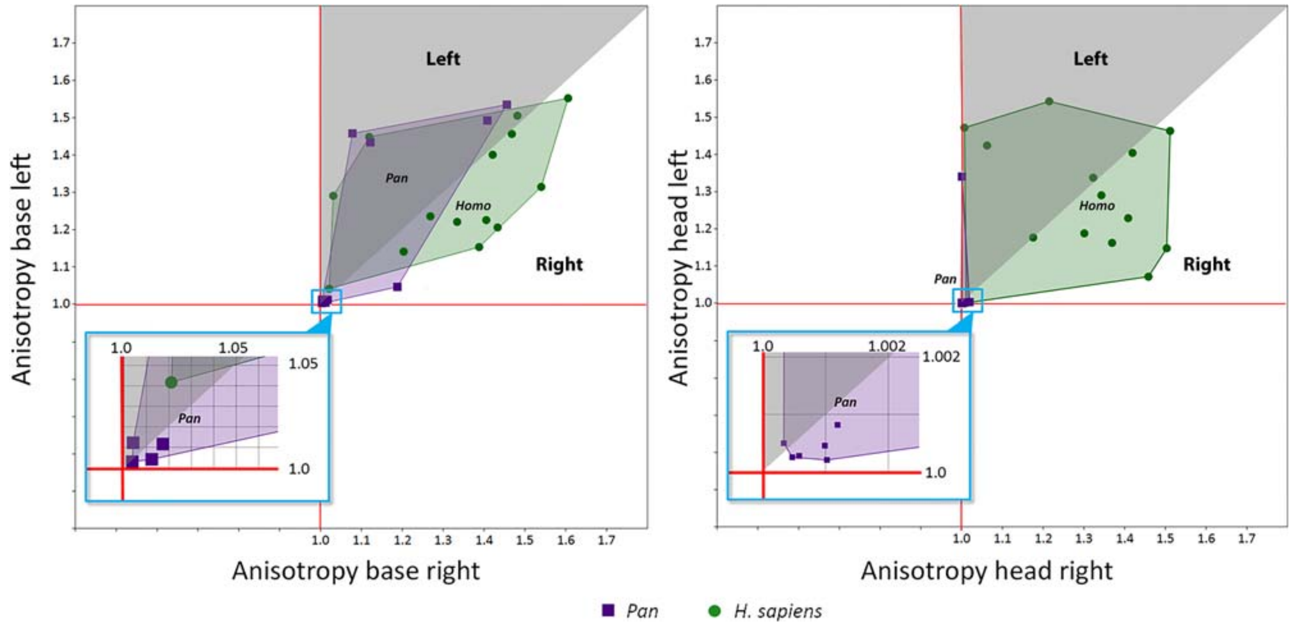

COLOR

**FIGURE 2** Degree of anisotropy of the first metacarpal base (left) and head (right) for both sides of each individual. The shaded area indicates individuals demonstrating a left directional asymmetry while the red line indicates isotropy. *H. sapiens* (green dot) variation in anisotropy for both regions, while *Pan* (purple square) is very constrained. The blue box is a magnified view of clustered individuals that approach total isotropy for both sides. This is particularly marked in the head of *Pan*, with six individuals contained between 1.0 and 1.002 on both sides

biomechanical environment and, because of this; (2) the directional asymmetry of trabecular architectural variables (i.e., greater BV/TV, DA, and elastic modulus) in H. sapiens will be significantly greater on the right; (3) while Pan will exhibit no significant departure from a neutral (50%) distribution.

## 2 | MATERIALS AND METHODS

### 2.1 | Study sample

The H. sapiens Mc1 sample ($n = 14$ pairs) is composed of ten $1^{st}-3$rd century CE individuals from the Roman necropolis of Isola Sacra (Italy) (Prowse et al., 2008), two 19th century individuals from Tiera del Fuego (Chile/Argentina) (Marangoni et al., 2011), and two 20th century individuals from Syracuse (Sicily). The Pan cohort ($n = 9$ pairs) is composed of four wild-shot individuals from southern Cameroon (Pan troglodytes spp.), three wild individuals from Côte d'Ivoire (Pan troglodytes verus) and two wild-shot individuals from the Congo Basin (DRC) (Pan paniscus).

### 2.2 | Micro-CT scanning and tissue segmentation

The heads and bases of the paired Mc1 remains from Isola Sacra and Côte d'Ivoire were scanned without the metaphyses (as part of a previous study) with a Skyscan (Aartselaar, Belgium) 1172 desktop Micro-CT scanner at an isotropic voxel resolution of 13.56 μm (parameters: 100 kV, 0.094 mA, 0.5-mm aluminum filter, 0.25 rotation step, 360 degrees of rotation, with two frame averaging). The remaining Mc1s

AQ6 **TABLE 2** Right/left count comparisons within and between groups

| | *Pan* ($n = 9$) | | | *Homo* ($n = 14$) | | | Between groups | |
|---|---|---|---|---|---|---|---|---|
| Variable | R>L | DIRA, % | *B* | R>L | DIRA, % | *B* | $\chi^2$ | *p* Value |
| BV/TV head | **1/9** | −5.94 | **0.039** | 10/14 | 11.95 | 0.179 | **7.987** | **.005** |
| BV/TV base | 3/9 | −1.38 | 0.508 | **12/14** | 12.64 | **0.013** | **6.626** | **.010** |
| DA head | 7/9 | −2.93 | 0.180 | 9/14 | 1.01 | 0.424 | 0.471 | .493 |
| DA base | 4/9 | −5.80 | 1 | 10/14 | 2.57 | 0.180 | 1.675 | .196 |
| *E* head | 2/9 | −10.94 | 0.180 | 11/14 | 23.15 | 0.057 | **7.078** | **.008** |
| *E* base | 4/9 | −2.54 | 1 | **12/14** | 22.32 | **0.013** | 4.407 | **.036** |

Abbreviations (BV/TV = bone volume; DA = degree of anisotropy; *E* = elastic modulus in gigapascals; R > L = # of individuals displaying right directional asymmetry; DIRA = average direction of asymmetry with negative numbers indicating a left directional asymmetry; B = *p* values for binomial exact test for deviations from an expected 50/50 distribution; $\chi^2$ = *p* values for Pearson's $\chi^2$ test to determine if directional asymmetry counts between groups are significantly different).

**TABLE 3** Average absolute asymmetry within and between groups

| Variable | *Pan* (*n* = 9) AA, % | *Homo* (*n* = 14) AA, % | Between groups *U* | *p* Value |
|---|---|---|---|---|
| BV/TV head | 5.99 | 16.21 | 20.00 | **.005** |
| BV/TV base | 6.44 | 14.74 | 34.00 | .072 |
| DA head | 3.52 | 14.11 | 16.00 | **.002** |
| DA base | 8.95 | 9.95 | 50.00 | .439 |
| *E* head | 11.84 | 29.82 | 27.00 | **.023** |
| *E* base | 11.14 | 26.24 | 34.00 | .068 |

Abbreviations (BV/TV = bone volume; DA = degree of anisotropy; *E* = elastic modulus; AA = mean absolute asymmetry; *U* = Mann–Whitney *U* score; *p* = exact *p* value for Mann–Whitney *U* test).

were scanned in their entirety with a BIR ACTIS 225/300 high-resolution Micro-CT scanner at an isotropic voxel resolution ~30 µm (parameters: 130 kV and 100 IA using a 0.25 aluminum filter). The heads and bases of the complete Mc1 sample were isolated and cropped using Avizo 6.3 to allow for uniform comparison with those scanned without the metaphysis. Segmentation of bone tissue in each scan was accomplished using the Ray Casting Algorithm of Scher and Tilgner (2009).

## 2.3 | Trabecular bone analysis and visualization

Unless noted otherwise, all procedures were performed with medtool (Dr. Pahr Ingenieurs e.U.). After segmentation, trabecular and cortical bone were isolated using protocols outlined in Gross et al. (2014). In brief, opening-and-closing filters (kernel size = 3) were employed to remove natural cortical porosities, which permits creation of a smooth shell that is then filled to create an inner- and outer-mask of the whole bone. The resultant cortical mask is then used to create an independent image of each tissue. This process is repeated, to replace the initial kernel size with one taking into account the average trabecular thickness measured by the BoneJ plugin (Doube et al., 2010) in ImageJ (Rasband, 1997; see also Gross et al., 2014).

We focus our analysis of asymmetry in trabecular structure on three variables: average bone volume to total volume fraction (BV/TV), degree of anisotropy (DA), and the elastic modulus (*E*), which is measured in gigapascals (GPa) (Pahr and Zysset, 2009). These variables were chosen because it has been demonstrated that body mass does not strongly correlate with BV/TV or DA (Barak, Lieberman, & Hublin, 2013; Doube, Klosowski, Wiktorowicz-Conroy, Hutchinson, & Shefelbine, 2011; Ryan & Shaw, 2013), and that they have a well-established correlation with mechanical loading and functional bone adaptation (Barak et al., 2011; Lambers, Bouman, Rimnac, & Hernandez, 2013; Odgaard, 1997; Pontzer et al., 2006; Uchiyama et al., 1999). Although the relationship between trabecular structure and *E* depends on the anatomical location and direction of loading (Morgan, Bayraktar, & Keaveny, 2003), it is an accepted proxy for bone strength (Helgason et al., 2008; Stauber et al., 2006). Herein we calculate *E* following the Zysset-Curnier model (Zysset, 2003) using a reference tissue value of $E0 = 10$ GPa; $\nu0 = 0.3$; $\mu0 = 3$ GPa, because it takes into account BV/TV and mean intercept length derived fabric, which has been demonstrated in several anatomical locations to be a better predictor of the mechanical properties of trabecular bone (~97%) than other models (Haïat et al., 2009; Maquer et al., 2015).

To analyze each variable throughout the epiphyseal head and base of each Mc1, a 5 mm spherical VOI was passed over a rectangular 2.5 mm 3D grid placed over the trabecular mask. From these VOIs,

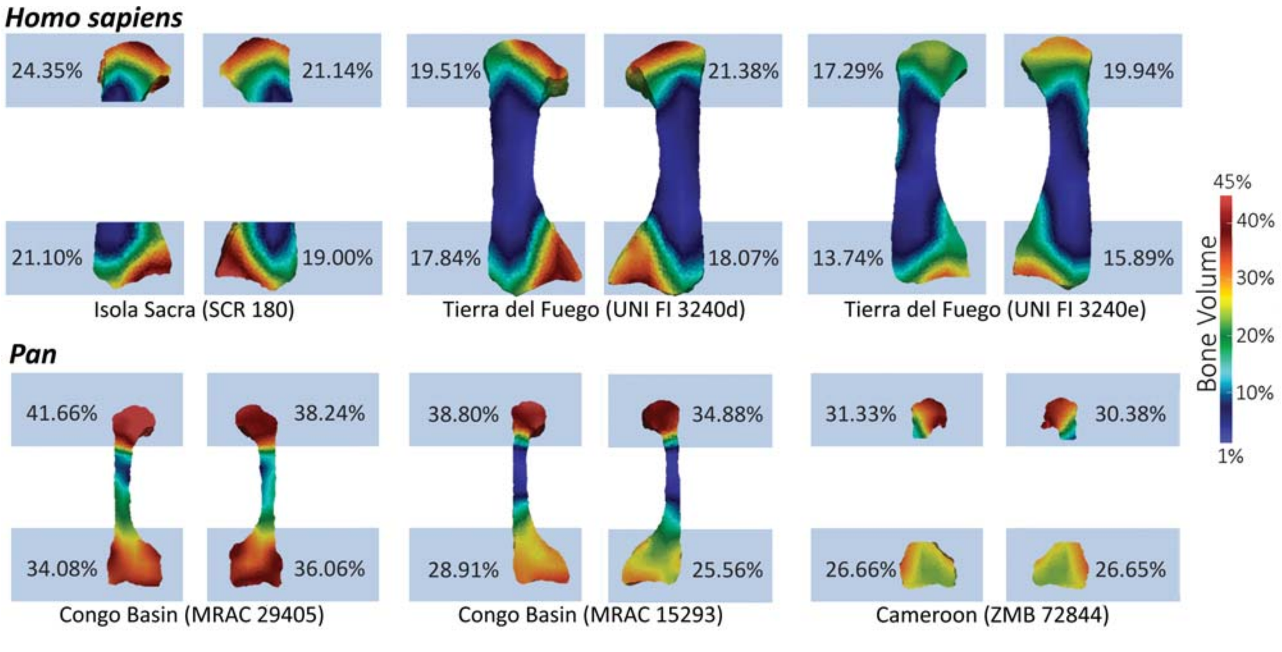

**FIGURE 3** Mid-sagittal cross section of right and left first metacarpals exemplifying the site specific internal distribution and average bone volume for *H. sapiens* (top) and *Pan* (bottom). Average quantitative BV/TV (%) for the head and base are indicated in the shaded boxes

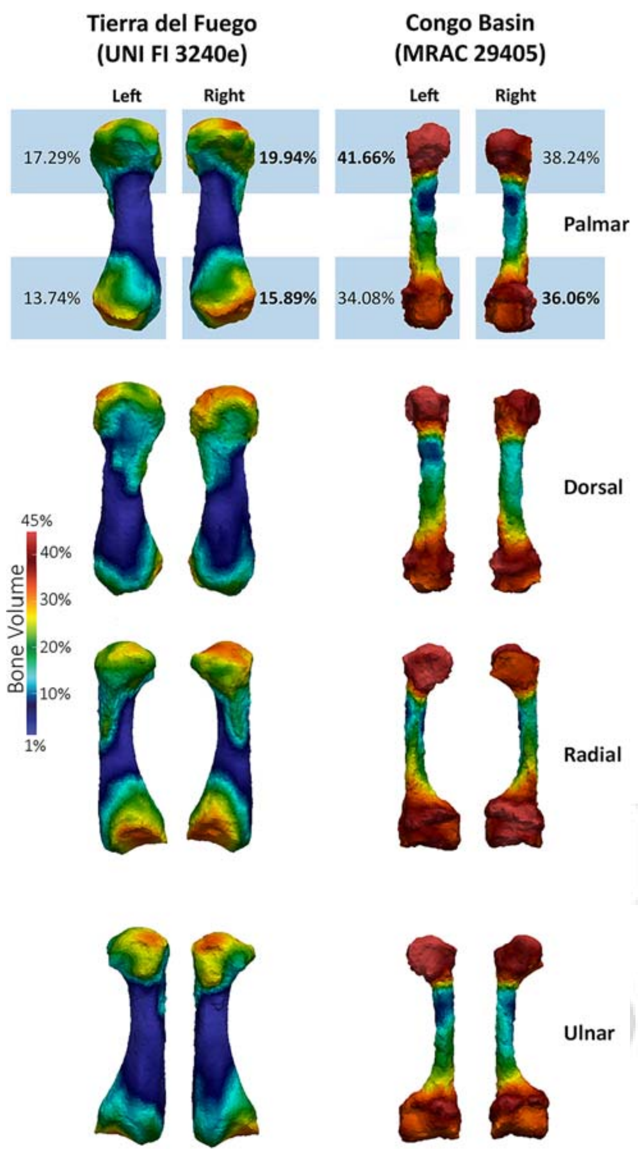

**FIGURE 4** 3D models showing the site specific BV/TV (%) distribution in the left and right first metacarpals in palmar, dorsal, radial, and ulnar views of a modern human (left) and a bonobo (right). Average quantitative BV/TV (%) for the head and base are indicated in palmar view with the greatest value from each side in bold

average values for each trabecular variable (BV/TV, DA, and *E*) within each epiphyseal segment were computed. To visualize and qualitatively compare the site-specific distribution of BV/TV, we first created a 3D tetrahedron mesh of the trabecular mask using HyperMesh® (Altair Engineering, Inc., USA), onto which we then mapped the BV/TV results from each VOI of the background grid analysis. These results were uniformly scaled between 1% and 45% and visualized using Paraview (v. 3.14.1, paraview.org), which allows the color-coded models of BV/TV to be viewed as complete trabecular mesh or by a user-defined 2D cross section.

## 2.4 | Calculation of asymmetry

Calculation of asymmetry follows the handedness index of Mays (2002) for directional asymmetry (DIRA): $\mathrm{DIRA} = (r - \mathrm{l})/((r + \mathrm{l})/2) \times 100$, where a positive number indicates right directional asymmetry (r) and a negative number left directional asymmetry (l). Similarly, absolute asymmetry (AA) is calculated by: $\mathrm{AA} = |r - \mathrm{l}|/((r + \mathrm{l})/2) \times 100$, with the difference being a standardized measure of the magnitude of asymmetry for comparison between groups (Palmer, 1994). Statistical analysis of the resulting variables was performed using SPSS 20 (IBM), R version 3.1.0, and PAST 3.04 (Hammer, Harper, & Ryan, 2001). Mann–Whitney *U* tests were used to determine if the values for the left/right variables differed significantly between Pan and Homo. Within-group exact binomial tests were performed on DIRA counts to determine if Pan and Homo departed from an expected 50/50 right- versus left-distribution, while Pearson's $\chi^2$ tests were performed to determine if these counts differed significantly between the two groups. Mann–Whitney *U* tests were performed to determine if absolute asymmetry values differed significantly between the two groups.

# 3 | RESULTS

## 3.1 | Quantitative results

Averages and standard deviations for the mean (sides combined) and side-specific (i.e., right and left) trabecular variables (BV/TV, DA, and *E*) for the Pan and H. sapiens groups are shown in Table 1. On average, Pan exhibits left directional asymmetry and H. sapiens exhibit a right-directional asymmetry for each variable at the head and base. Mann–Whitney *U* tests are significant between Pan and H. sapiens for all variables, with Pan being considerably more isotropic and having greater overall BV/TV and *E* for both regions. It is also evident that Pan and H. sapiens share a distinct difference in the pattern of trabecular variables at the head and base, with the Mc1 head having greater BV/TV and *E* but lower DA when compared with the base. Figures 1 and 2 present bi-variate plots of BV/TV and DA distribution in each epiphysis. As noted above, Pan has greater BV/TV in both the head and base and a greater number of individuals that exhibit a left directional asymmetry (see below). Although there is overlap between the two groups in DA values at the Mc1 base, the majority of Pan individuals approach isotropy (DA close to 1) on both sides at the head.

Table 2 presents the results of DIRA and right directional asymmetry individual counts, along with results from the within-group binomial exact and between-group $\chi^2$ tests. The binomial exact tests found that the right directional asymmetry for H. sapiens is significant at the Mc1 base for BV/TV and *E*, while the left directional asymmetry for Pan is significant at the head for BV/TV. The between groups $\chi^2$ tests found that the right directional asymmetry count distribution was significantly different from the expected 50/50 right versus left distribution for BV/TV and *E* for both the Mc1 head and base. These differences in frequency can also be seen in Figures 1 and 2 for BV/TV and DA, respectively.

Table 3 presents the results of Mann–Whitney *U* tests for significant differences in absolute asymmetry between H. sapiens and Pan. BV/TV, DA, and *E* all exhibit significantly greater absolute asymmetry at the Mc1 head, but not at the base.

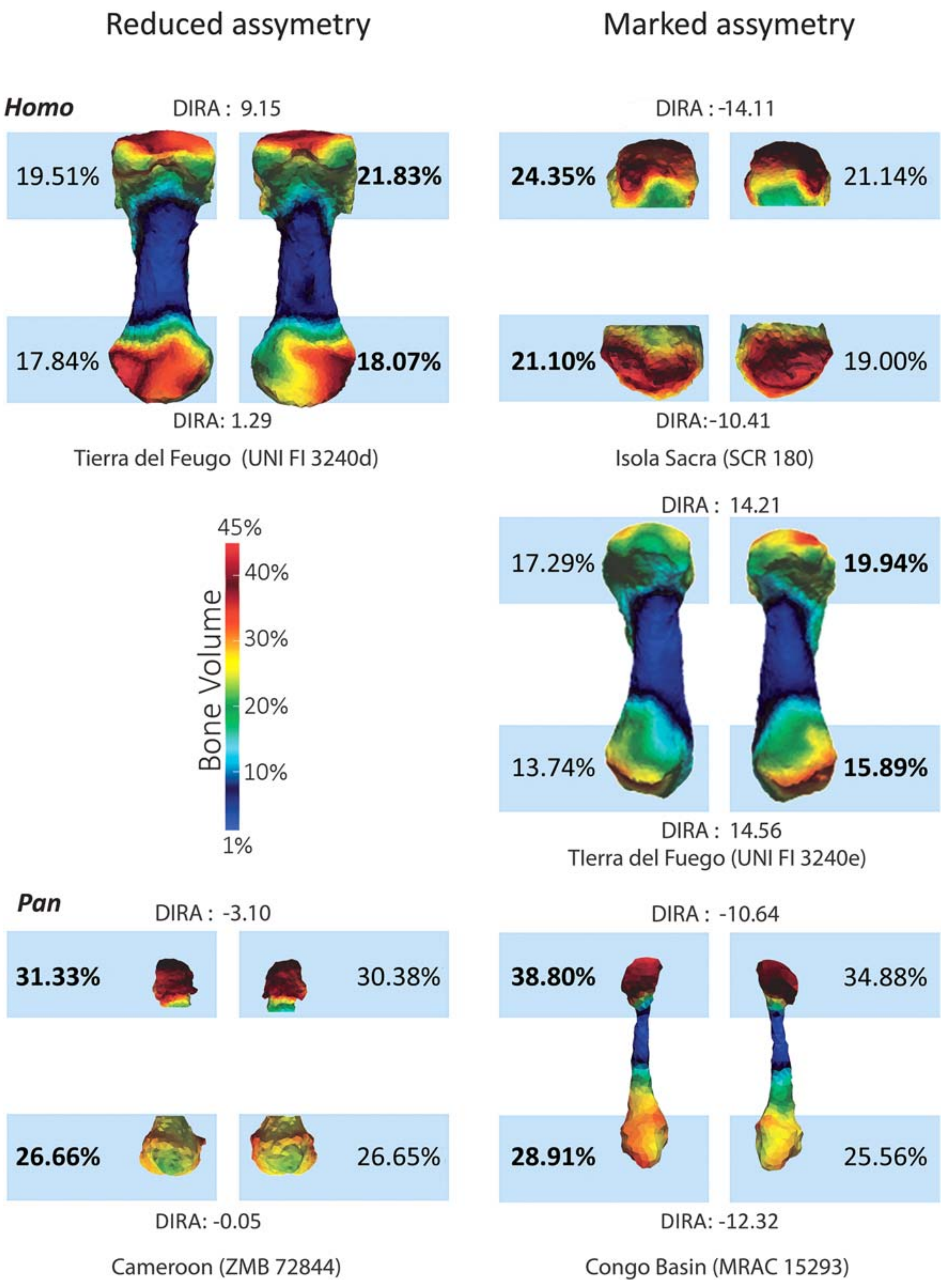

COLOR

**FIGURE 5** Representative 3D models of right and left first metacarpals BV/TV (%) and levels of directional asymmetry (DIRA). The greater average BV/TV for the region indicated by the shaded boxes are in bold. Individuals with a left directional asymmetry are indicated by a negative number, while those with right directional asymmetry are indicated by a positive number

## 3.2 | Qualitative results

Figure 3 is a mid-sagittal cross section exemplifying the site-specific internal bone volume distribution and individual quantitative averages at the Mc1 head and base for a selection of H. sapiens and Pan while Figure 4 is an external view (i.e., complete trabecular mesh). The differences in site-specific bone volume concentration and distribution are reflected in the color maps, and illustrate that the Pan sample is more

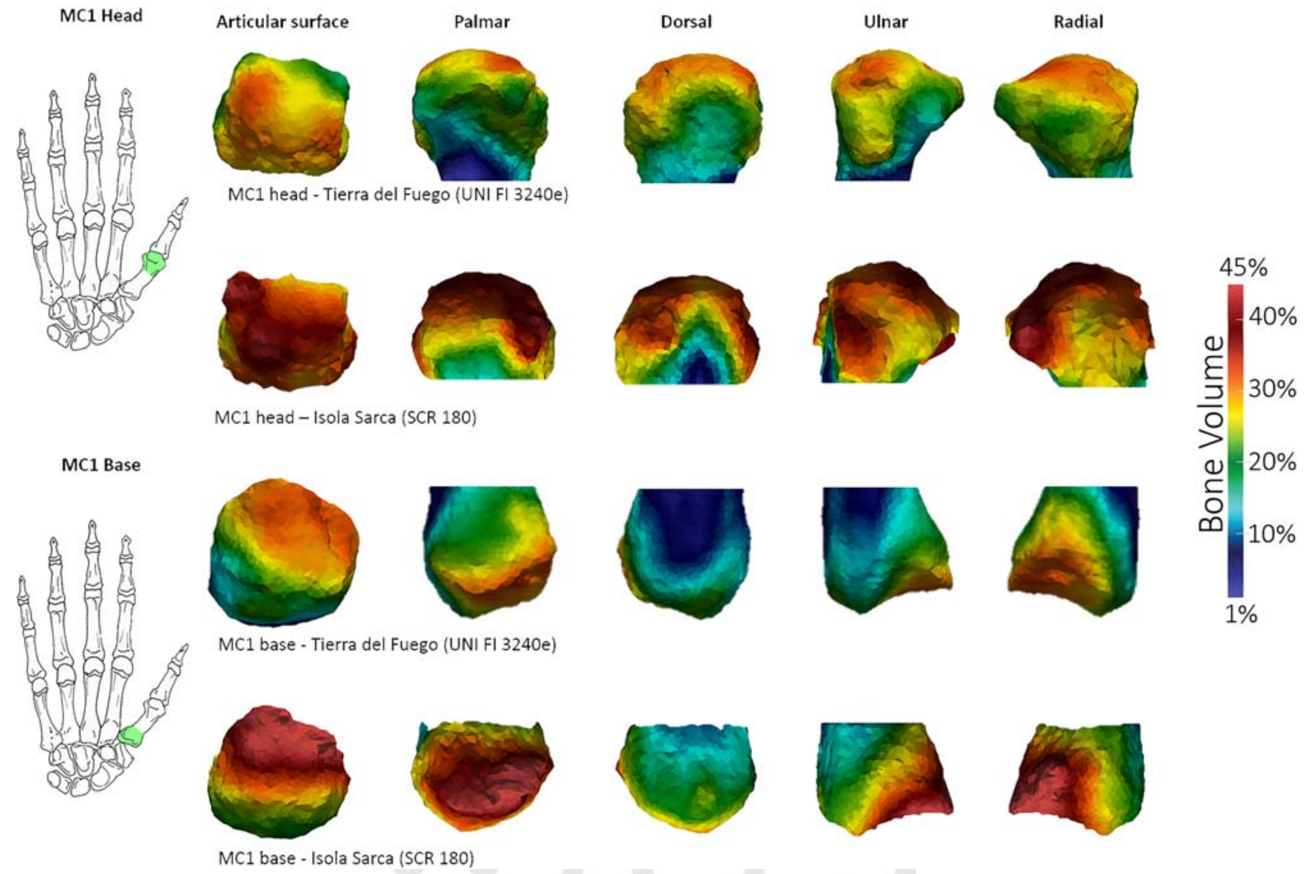

**FIGURE 6** Example of site specific bone volume distribution in the first metacarpal head (top two rows) and base (bottom two rows) for two *H. sapiens* individuals (SCR 180 and UNI FI 3240e)

uniform internally in both Mc1 regions, while concentrations in the H. sapiens are found towards the articular surface areas. Also of note are the variations in distribution between left and right sides, with a greater radial concentration at the right base and head in the individual from Tierra del Fuego (UNI FI 3240e, Figures 3 and 4).

Figure 5 shows examples of low and marked directional asymmetry for representative H. sapiens and Pan. Herein the complexity of determining asymmetry is made clear because although the bone volume quantitative averages provide evidence for a right or left directional asymmetry, the concentrations and uniformity do vary between the head and base regions (e.g., MRAC 15293 compared with ZMB 72844). Furthermore, site-specific distribution and concentration of bone volume also varies between individuals (UNI FI 3240d base, see also cross section in Figure 3). For example, in certain Pan (MRAC 29045) individuals the right/left directional asymmetry is unclear, with the head being greater on the right directional but greater on the left at the base or vice versa.

Figure 6 shows the right Mc1 head and base for two H. sapiens individuals (UNI FI 3240e and SCR 180) in standard anatomical views. Even with different average values for each individual, the site-specific BV/TV pattern in H. sapiens shows that the trabecular distribution at the head is fairly concentrated at the articular surface, with the greatest volumes found at the contact areas for the first proximal phalanx. This is also the case at the base, but the highest concentrations are found at the palmar aspect of the articular surface and extend distally along the radial side.

Figure 7 shows the site-specific bone volume distribution for the right Mc1 head and base for two Pan individuals (MRAC 29045 and ZMB 72844) from standard anatomical views. The cause for the much higher average quantitative BV/TV is evident here, as the trabeculae are much more evenly distributed and palmarly concentrated throughout the head. This is not as marked at the base where the greatest concentrations are not actually at the articular surface, but are instead slightly distal to the surface on the dorsal, ulnar, and radial sides, which contrasts with the pattern found at the H. sapiens Mc1 head and base (Figure 6).

## 4 | DISCUSSION

We sought to test whether skeletal asymmetries in trabecular bone were consistent with the assumption of increased mechanical loading on the dominant limb, following the mechanostat model of bone functional adaptation (Frost, 1987). Overall we found that the right directional asymmetry in measured epiphyseal trabecular variables of the paired first metacarpals (Mc1) from H. sapiens matched expectations, while the left directional asymmetry of Pan countered our expectations. We also report that, compared with Pan, H. sapiens have significantly lower bone volume (BV/TV) and elastic modulus (*E*), but higher

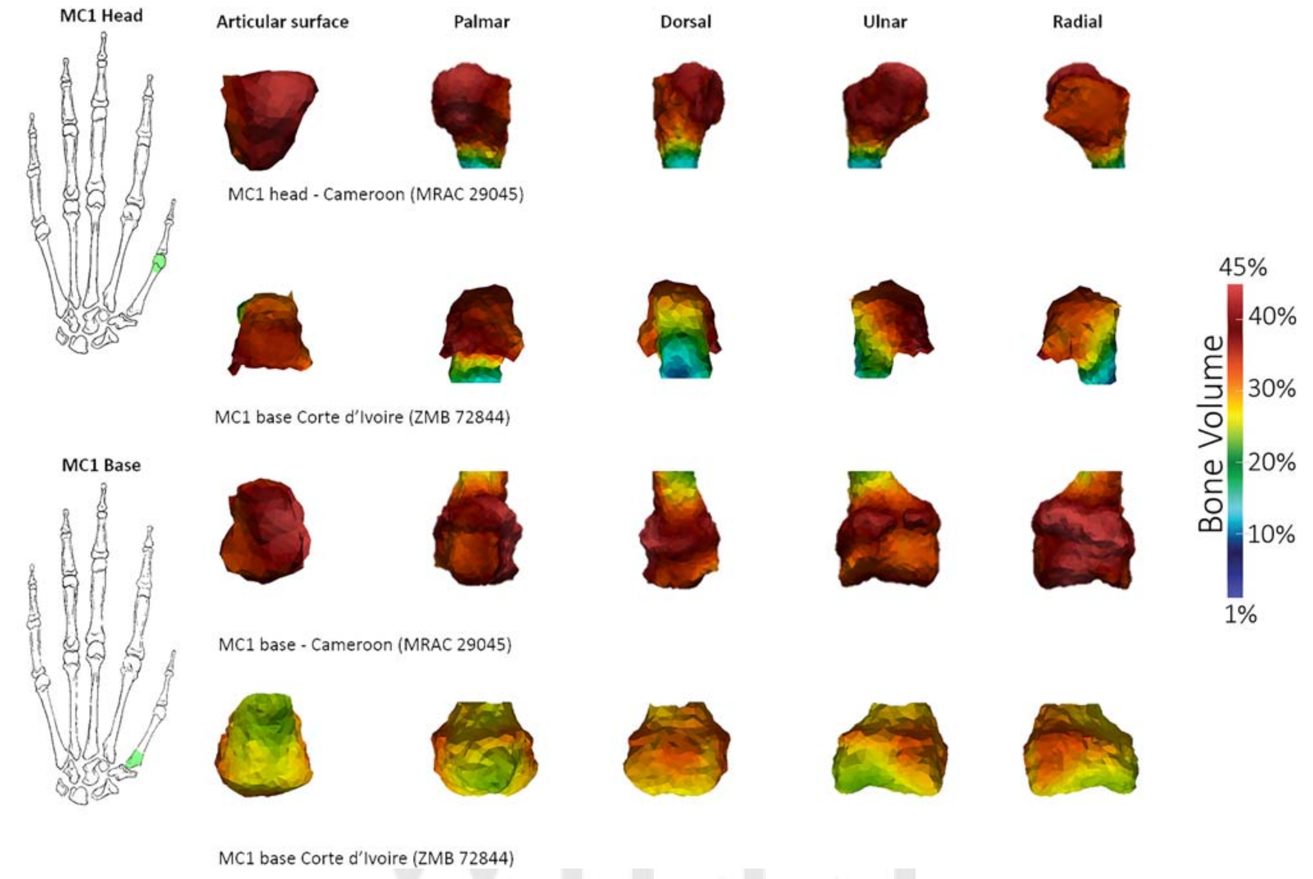

C
O
L
O
R

**FIGURE 7** Example of site specific bone volume distribution in the first metacarpal head (top two rows) and base (bottom two rows) for two *Pan* Individuals (MRAC 29045 and ZMB 72844)

degree of anisotropy (DA) in both regions. There is also a consistent head/base pattern evident in H. sapiens and Pan, with higher DA but lower BV/TV and *E* at the Mc1 base compared with the head. The individual site-specific BV/TV distribution models make it clear that many of the quantitative results are explained by the individual variation in the distribution of trabeculae, and suggest that the relationship between hand preference and directional asymmetry in the Mc1 epiphyseal trabecular architecture is not as straightforward as initially hypothesized.

## 4.1 | Directional asymmetry in *Homo sapiens*

In counts of right or left directional asymmetry we found a significant right directional asymmetry in BV/TV and *E* in the H. sapiens Mc1 base, while the Pan Mc1 reached a significant left directional asymmetry for BV/TV at the head. Comparisons between the two groups revealed that the counts reached significance for bone volume in both regions and elastic modulus at the base. Finally, H. sapiens displayed greater levels of absolute asymmetry for all trabecular variables in both regions with significant differences between the two groups existing at the Mc1 head.

We consider statistically significant greater trabecular variables (BV/TV and *E*) in the Mc1 base as the best indicator of loading related to hand preference. This appears to be supported by the palmar and radial bone volume concentrations at the articular surface, which conform with areas of localized remodeling in response to mechanical stimuli (Christen et al., 2014; Cresswell et al., 2016; Schulte et al., 2013) and speak to loading during flexion and forceful opposition (Ladd et al., 2014). These results join those of Lazenby, Angus, Cooper, and Hallgrimsson (2008) and Lazenby, Cooper, et al. (2008), who examined the directional asymmetry in paired second metacarpals and found a significant right directional asymmetry for trabecular bone volume at the head, mid-shaft cross-sectional geometry of the cortex, and mediolateral articular dimensions.

AQ2

## 4.2 | Directional asymmetry in *Pan*

We predicted that there would be no directional asymmetry detected in the Pan Mc1s because the thumb is removed from loading during lateralized terrestrial locomotion (Arcadi & Wallauer, 2011) and that other potential behaviors that produce asymmetrical loading of the thumb (e.g., arboreal locomotion, tool use) would not be detected at a group level. Our results did not support this prediction and instead we found a left directional asymmetry trend in the Pan Mc1. This result is not consistent with previous studies of Pan trabecular bone (Lazenby et al., 2011) that did not find any directional asymmetry. If the left directional asymmetry found in this study is a byproduct of manipulation, it is inconsistent with wild observational data that indicate only individual-level, but not group-level, hand preference (Boesch, 1991; Marchant & McGrew, 2007; McGrew & Marchant, 1992, 1997). Although the mechanostat model is admittedly oversimplified, it seems unlikely that variation in hormonal, genetic, and cellular responses across different anatomical regions could explain differences in right/left directional asymmetry within a single skeletal element. However, future studies could address this question, such as in a mouse model after Wallace et al. (2015), where right/left loading is controlled for as opposed to fore/hind limb.

We do, however, find a similar pattern to that reported here descried in a cortical bone assessment of Sarringhaus, Stock, Marchant, and McGrew (2005) who found a left directional asymmetry in the humerii and right directional asymmetry in the second metacarpals of P. troglodytes. They discussed a tradeoff in loading environments based on observations of wild chimpanzees (Hunt, 1991), where preference for manual support of the left-hand leaves the right free to collect food (Sarringhaus et al., 2005). Such a preference is noted in captive groups, with a left-hand preference existing for hanging (Morcillo, Fernandez-Carriba, & Loeches, 2006) and during front-forward descent, where the palm makes direct contact with the substrate (Hopkins, 2008). These observations are paired with studies of chimpanzee soft tissue anatomy that have found greater muscle mass on the left upper limb and greater muscle moment arms on the right (Carlson, 2006). These studies suggest that there may be greater asymmetry in Pan upper limb use and loading than previously thought, which could override signals of hand preference during manipulation and complicate direct comparisons between Pan and H. sapiens. Clarification of this issue requires the incorporation of more than a single skeletal element or osseous tissue. In the absence of such a comparison in the current study, we suggest that the homogenous distribution of bone volume, high elastic modulus, and near total isotropy in the Pan Mc1 is better explained by lateralized loading during locomotion and postural support. Given our finding of overall less absolute asymmetry in the Pan Mc1 in relation to that of H. sapiens, this type of lateralized loading appears more balanced, but implies that questions pertaining to skilled tool use and hand preference may only be appropriate for committed terrestrial bipeds.

## 4.3 | Mc1 loading in *Homo sapiens*

Compared with other primates, the low BV/TV of H. sapiens reported here agrees with reports of less dense trabecular architecture in humans in other skeletal elements (Chirchir et al., 2015; Griffin et al., 2010; Maga et al., 2006; Ryan & Shaw, 2012, 2013, 2015), including the hand (Schilling et al., 2013; Tsegai et al., 2013). The thumb has been described as operating as a single functional unit during flexion (Ladd et al., 2014), such that the three phalanges, trapezium, and supporting thenar musculotendon network act in concert to rotate and support the distal pad during the forceful opposition of the other fingers and/or manipulated objects (Brand & Hollister, 1993; Diogo et al., 2012; Landsmeer, 1955; Li & Tang, 2007; Marzke et al,. 1999). Our finding of greater BV/TV and *E* at the head relative to the base suggests that the Mc1 head experiences greater loading, but this may also be a result of loads being transferred into the broad surface of the trapezium (Marzke, 2013). Visually, the site-specific BV/TV concentrations at the articular surface of the head and palmar-radial concentration at the base are consistent with loads incurred while using a flexed and abducted thumb (e.g., key/pinch/power grips), where the base of the first metacarpal translates ulnarly and the radial articular surface resists the load (Halilaj et al., 2014). Such an interpretation also appears consistent with clinical micro-CT trabecular studies, which report a mirrored palmar-ulnar concentration in the trapezium that is thought to be an indication of remodeling in response to the axial displacement of force during thumb loading (Ladd et al., 2014; Lee et al., 2013; Nufer et al., 2008). As such, this pattern appears to be biomechanically consistent between bones, but would benefit by having a broader comparison of trabecular structure across the remaining bones of the hand.

## 4.4 | Mc1 loading in *Pan*

We find that the high BV/TV, low DA, and head/base pattern reported for Pan Mc1s here agrees with results derived from a similar Mc1 sample using single VOIs by Lazenby et al. (2011). A strict interpretation of the mechanostat model would suggest that the extremely high BV/TV and *E* in the Pan Mc1, when compared with H. sapiens, is a direct result of high impact mechanical loading. This pattern would be consistent with the scenario described above, where the high BV/TV and *E* in the Pan Mc1 compensate for the reduced thenar musculature (Diogo et al., 2012; Marzke et al., 1999) and smaller joint surfaces in the thumb complex (Marzke, 2013) during locomotion and postural support. However, as discussed above, bone functional adaptation is a complex aspect of biology and our results are not inconsistent with a view that systemic differences in hormones, genes (Paternoster et al., 2013; Wallace et al., 2010; Yerges et al., 2010), and cellular response to loading (Wallace et al., 2015) may also work to explain the genera-level differences reported here. This being the case, a one-to-one correlation between loading and bone morphology is not supported by our results and, we can only suggest that the greater BV/TV and *E* in the Pan Mc1 are byproducts of systemic hormonal/genetic differences in combination with loading.

Even so, evidence for localized loading and bone remodeling does exist in the site-specific areas of high BV/TV concentration in the Pan Mc1 base, visible just above the articular surface. These regions appear correspondent with the muscle attachment sites responsible for flexion of the thumb (Diogo, Potau, & Pastor, 2013; Marzke et al., 1999). This is intriguing in light of the report of Marzke et al. (2015), who recognized previously unobserved hand grips during food processing that appear to involve forceful loading of the thumb. These include a thrusting movement involving large fruits held in the pocket between the thumb and index, and a variation of the transverse hook grip that depends on leverage provided by the thumb to strip away meat clenched between teeth. Although this result suggests that the relationship between muscle attachment sites and trabecular response requires additional exploration, the uniformity of bone volume, extremely low anisotropy, and high elastic modulus speaks to a greater demand for multi-axial loading than manipulation or feeding alone. Being that these grips are also observed during arboreal locomotion, which is very complex and variable throughout life (Sarringhaus et al., 2014), our results are perhaps best explained by loading during contact with a highly variable substrate. If this interpretation is correct, then it implies that the signal from subtler loading scenarios, such as those during manipulation, may be reduced or lost in favor of loading regimes with higher peak loading.

## 5 | CONCLUSION

In summary, we found that the first metacarpal trabecular pattern and distribution were consistent with the biomechanical role of the thumb and found that counts of right directional asymmetry for average bone volume and elastic modulus at the base reached significance, which appears to be concordant with the 85–95% right-hand preference reported cross-culturally. Contrary to our expectations we also found a significant left directional asymmetry at the Pan Mc1 head for bone volume that, combined with the finding of extremely low DA and high *E* in both head/base regions, is best explained as a reflection of individual preference for left side lateralized loading during locomotion and postural support. We also report greater BV/TV and *E* in the Pan Mc1, when compared with H. sapiens, which we stress is likely a reflection of a systemic hormonal/genetic difference between the two groups and is likely not an indication of greater loading in the Pan thumb. This is an important consideration that should be kept in mind during the analysis and interpretation of hominin fossil remains (see discussion in Wallace et al., 2015). As such, we suggest that behavioral studies concerned with the manifestations of bone functional adaptation should adopt a layered analysis that incorporates multiple techniques to check the biomechanical agreement of various osseous tissues and taxa.

To conclude, we found directional asymmetry in the first metacarpal trabecular architecture, but caution that the cause of this bias is not always a clear indication of individual hand preference during manipulative tasks and suggest that additional analyses be applied to multiple skeletal elements and other osteological features (e.g., cortical bone) whenever possible. We also found that our interpretation of the quantitative results and potential loading histories were greatly aided by referring to the site-specific bone volume distribution models. As such, our analysis builds upon previous studies that have used trabecular architecture to investigate loading history and its relationship to bone functional adaptation. We conclude the characterization and visualization of trabecular architecture is a method that should be joined with previously established techniques to supplement fossil studies concerned with the evolution of handedness. Such an application has great potential to provide missing information prior to the advent of stone tool manufacture, and would thus improve our understanding of the hypothesized cause and effect relationship between knapping, brains, and behavior.

## ACKNOWLEDGMENTS

We are grateful for the samples provided by Berlin Museum für Naturkunde (Frieder Mayer), Max Planck Institute for Evolutionary Anthropology (Christophe Boesch), Musée Royal de l'Afrique Centrale (Emmanuel Gilissen), Museo Nazionale Preistorico Etnografico "Luigi Pigorini" (Roberto Macchiarelli), Naturhistorisches Museum Wien (Maria Teschler-Nicola, Ronald Muehl), Senckenberg Museum (Virginie Volpato), and University of Florence (Jacopo Moggi-Cecchi and Silvia Bortoluzzi). For scanning assistance we thank Patrick Schoenfeld and Heiko Temming. For discussions we thank Zewdi Tsegai, Kellie Sara Duffett Carlson, Adam Van Casteren, and Robi Sen. This research was supported by the Max Planck Society (NBS, MMS, TLK, JJH, NHN) and the European Research Council Starting Grant #336301 (TLK and MMS).

## REFERENCES

AQ7

Almécija, S., Alba, D. M., & Moya-Sola, S. (2012). The thumb of Miocene apes: New insights from Castell de Barbera (Catalonia, Spain). *American Journal of Physical Anthropology*, *148*, 436–450.

Almécija, S., Wallace, I. J., Judex, S., Alba, D. M., & Moya-Sola, S. (2015). Comment on "Human-like hand use in *Australopithecus africanus*". *Science*, *348*, 1101–1101.

AQ3

Andrew, R. J., & Rogers, L. J. (2002). The nature of lateralization in tetrapods. In L. J. Rogers & R. J. Andrew (Eds.), *Comparative vertebrate lateralization* (pp. 94–125). Cambridge, UK: Cambridge University Press.

Arcadi, A. C., & Wallauer, W. (2011). Individual-level lateralization in the asymmetrical gaits of wild chimpanzees (Pan troglodytes): Implications for hand preference and skeletal asymmetry? *Behaviour*, *148*, 1419–1441.

Armour, J. A., Davison, A., & McManus, I. C. (2014). Genome-wide association study of handedness excludes simple genetic models. *Heredity (Edinb)*, *112*, 221–225.

Auerbach, B. M., & Ruff, C. B. (2006). Limb bone bilateral asymmetry: Variability and commonality among modern humans. *Journal of Human Evolution*, *50*, 203–218.

Bahtiri, E., Islami, H., Rexhepi, S., Qorraj-Bytyqi, H., Thaci, K., Thaci, S., . . . Hoxha, R. (2015). Relationship of homocysteine levels with lumbar spine and femur neck BMD in postmenopausal women. *Acta Reumatologica Portuguesa*, *40*, 355–362.

Barak, M. M., Lieberman, D. E., & Hublin, J. J. (2011). A Wolff in sheep's clothing: Trabecular bone adaptation in response to changes in joint loading orientation. *Bone*, *49*, 1141–1151.

Barak, M. M., Lieberman, D. E., & Hublin, J. J. (2013). Of mice, rats and men: Trabecular bone architecture in mammals scales to body mass with negative allometry. *Journal of Structural Biology*, *183*, 123–131.

Barak, M. M., Lieberman, D. E., Raichlen, D., Pontzer, H., Warrener, A. G., & Hublin, J. J. (2013). Trabecular evidence for a human-like gait in *Australopithecus africanus*. *PLoS One*, *8*, e77687.

Bardo, A., Pouydebat, E., & Meunier, H. (2015). Do bimanual coordination, tool use, and body posture contribute equally to hand preferences in bonobos? *Journal of Human Evolution*, *82*, 159–169.

Barros, A., & Soligo, C. (2013). Bilateral asymmetry of humeral torsion and length in African apes and humans. *Folia Primatologica (Basel)*, *84*, 220–238.

Bass, S. L., Saxon, L., Daly, R. M., Turner, C. H., Robling, A. G., Seeman, E., & Stuckey, S. (2002). The effect of mechanical loading on the size and shape of bone in pre-, peri-, and postpubertal girls: A study in tennis players. *Journal of Bone and Mineral Research*, *17*, 2274–2280.

Bermúdez de Castro, J., Bromage, T. G., & Jalvo, Y. F. (1988). Buccal striations on fossil human anterior teeth: Evidence of handedness in the middle and early Upper Pleistocene. *Journal of Human Evolution*, *17*, 403–412.

Boesch, C. (1991). Handedness in wild chimpanzees. *International Journal of Primatology*, *12*, 541–558.

Boesch, C., & Boesch, H. (1993). Different hand postures for pounding nuts with natural hammers by wild chimpanzees. In H. Preuschoft & D. Chivers (Eds.), *Hands of primates* (pp. 31–43). Vienna: Springer.

Braccini, S., Lambeth, S., Schapiro, S., & Fitch, W. T. (2010). Bipedal tool use strengthens chimpanzee hand preferences. *Journal of Human Evolution*, *58*, 234–241.

Brand, P. W., & Hollister, A. (1993). *Clinical mechanics of the hand*. St. Louis, MO: Mosby Year Book.

Byrne, R. W., & Byrne, J. M. (1991). Hand preferences in the skilled gathering tasks of mountain gorillas (*Gorilla g. beringei*). *Cortex*, *27*, 521–546.

Cantalupo, C., Freeman, H., Rodes, W., & Hopkins, W. (2008). Handedness for tool use correlates with cerebellar asymmetries in chimpanzees (Pan troglodytes). *Behavioral Neuroscience*, *122*, 191–198.

Carlson, K. J. (2006). Muscle architecture of the common chimpanzee (Pan troglodytes): Perspectives for investigating chimpanzee behavior. *Primates*, *47*, 218–229.

Cashmore, L., Uomini, N., & Chapelain, A. (2008). The evolution of handedness in humans and great apes: A review and current issues. *Journal of Anthropological Sciences*, *86*, 7–35.

Cheema, T. A., Cheema, N. I., Tayyab, R., & Firoozbakhsh, K. (2006). Measurement of rotation of the first metacarpal during opposition using computed tomography. *Journal of Hand Surgery*, *31*, 76–79. (American Volume),

Chirchir, H., Kivell, T. L., Ruff, C. B., Hublin, J. J., Carlson, K. J., Zipfel, B., & Richmond, B. G. (2015). Recent origin of low trabecular bone density in modern humans. *Proceedings of the National Academy of Sciences of the United States of America*, *112*, 366–371.

Christen, P., Ito, K., Ellouz, R., Boutroy, S., Sornay-Rendu, E., Chapurlat, R. D., & van Rietbergen, B. (2014). Bone remodeling in humans is load-driven but not lazy. *Nature Communications*, *5*, 4855. AQ4

Churchill, S. E. (2001). Hand morphology, manipulation, and tool use in Neanderthals and early modern humans of the Near East. *Proceedings of the National Academy of Sciences of the United States of America*, *98*, 2953–2955.

Churchill, S. E., & Formicola, V. (1997). A case of marked bilateral asymmetry in the upper limbs of an upper palaeolithic male from Barma Grande (Liguria), Italy. *International Journal of Osteoarchaeology*, *7*, 18–38.

Corballis, M. C. (2003). From mouth to hand: Gesture, speech, and the evolution of right-handedness. *The Behavioral and Brain Sciences*, *26*, 199–208.

Cowell, P. E., Waters, N. S., & Denenberg, V. H. (1997). The effects of early environment on the development of functional laterality in Morris maze performance. *Laterality*, *2*, 221–232.

Cresswell, E. N., Goff, M. G., Nguyen, T. M., Lee, W. X., & Hernandez, C. J. (2016). Spatial relationships between bone formation and mechanical stress within cancellous bone. *Journal of Biomechanics*, *49*, 222–228.

Currey, J. D. (2003). The many adaptations of bone. *Journal of Biomechanics*, *36*, 1487–1495.

Currey, J. D. (2012). The structure and mechanics of bone. *Journal of Materials Science*, *47*, 41–54.

Demes, B., Stern, J. T., Jr., Hausman, M. R., Larson, S. G., McLeod, K. J., & Rubin, C. T. (1998). Patterns of strain in the macaque ulna during functional activity. *American Journal of Physical Anthropology*, *106*, 87–100.

Dempster, D. W., & Raisz, L. G. (2015). Bone physiology: Bone cells, modeling, and remodeling. In F. M. Holick & W. J. Nieves (Eds.), *Nutrition and bone health* (pp. 37–56). New York, NY: Springer.

Diogo, R., Potau, J. M., & Pastor, J. F. (2013). *Photographic and descriptive musculoskeletal atlas of chimpanzees: With notes on the attachments, variations, innervation, function and synonymy and weight of the muscles*. Boca Raton, FL: CRC Press.

Diogo, R., Richmond, B. G., & Wood, B. (2012). Evolution and homologies of primate and modern human hand and forearm muscles, with notes on thumb movements and tool use. *Journal of Human Evolution*, *63*, 64–78.

Dodson, D. L., Stafford, D., Forsythe, C., Seltzer, C. P., & Ward, J. P. (1992). Laterality in quadrupedal and bipedal prosimians: Reach and whole-body turn in the mouse lemur (Microcebus-Murinus) and the galago (Galago-Moholi). *American Journal of Primatology*, *26*, 191–202.

Doube, M., Klosowski, M. M., Arganda-Carreras, I., Cordelieres, F. P., Dougherty, R. P., Jackson, J. S., … Shefelbine, S. J. (2010). BoneJ: Free and extensible bone image analysis in ImageJ. *Bone*, *47*, 1076–1079.

Doube, M., Klosowski, M. M., Wiktorowicz-Conroy, A. M., Hutchinson, J. R., & Shefelbine, S. J. (2011). Trabecular bone scales allometrically in mammals and birds. *Proceedings of the Royal Society B: Biological Sciences*, *278*, 3067–3073.

Fajardo, R. J., & Müller, R. (2001). Three-dimensional analysis of nonhuman primate trabecular architecture using micro-computed tomography. *American Journal of Physical Anthropology*, *115*, 327–336.

Fajardo, R. J., Müller, R., Ketcham, R. A., & Colbert, M. (2007). Nonhuman anthropoid primate femoral neck trabecular architecture and its relationship to locomotor mode. *Anatomical Record*, *290*, 422–436.

Faurie, C., & Raymond, M. (2004). Handedness frequency over more than ten thousand years. *Proceedings of the Royal Society B: Biological Sciences*, *271*, S43–S45.

Faurie, C., Schiefenhovel, W., Le Bomin, S., Billiard, S., & Raymond, M. (2005). Variation in the frequency of left-handedness in traditional societies. *Current Anthropology*, *46*, 142–147.

Fitch, W. T., & Braccini, S. N. (2013). Primate laterality and the biology and evolution of human handedness: A review and synthesis. *Annals of the New York Academy of Sciences*, *1288*, 70–85.

Frayer, D. W., Lozano, M., Bermúdez de Castro, J. M., Carbonell, E., Arsuaga, J. L., Radovcic, J., … Bondioli, L. (2012). More than 500,000 years of right-handedness in Europe. *Laterality*, *17*, 51–69.

Frost, H. M. (1987). Bone “mass” and the “mechanostat”: A proposal. *The Anatomical Record*, *219*, 1–9.

Frühholz, S., Hofstetter, C., Cristinzio, C., Saj, A., Seeck, M., Vuilleumier, P., & Grandjean, D. (2015). Asymmetrical effects of unilateral right or left amygdala damage on auditory cortical processing of vocal emotions. *Proceedings of the National Academy of Sciences of the United States of America*, *112*, 1583–1588.

Griffin, N. L., D’aout, K., Ryan, T. M., Richmond, B. G., Ketcham, R. A., & Postnov, A. (2010). Comparative forefoot trabecular bone architecture in extant hominids. *Journal of Human Evolution*, *59*, 202–213.

Gross, T., Kivell, T. L., Skinner, M. M., Nguyen, N. H., & Pahr, D. H. (2014). A CT-image-based framework for the holistic analysis of cortical and trabecular bone morphology. *Palaeontologia Electronica*, *17*, 33A.

Haïat, G., Padilla, F., Svrcekova, M., Chevalier, Y., Pahr, D., Peyrin, F., . . . Zysset, P. (2009). Relationship between ultrasonic parameters and apparent trabecular bone elastic modulus: A numerical approach. *Journal of Biomechanics*, *42*, 2033–2039.

Halilaj, E., Rainbow, M. J., Got, C., Schwartz, J. B., Moore, D. C., Weiss, A. P., . . . Crisco, J. J. (2014). *In vivo* kinematics of the thumb carpometacarpal joint during three isometric functional tasks. *Clinical Orthopaedics and Related Research*, *472*, 1114–1122.

Hammer, Ø., Harper, D., & Ryan, P. (2001). Past: Paleontological statistics software package for education and data analysis. *Palaeontologia Electronica*, *4*, 1–9.

Harmand, S., Lewis, J. E., Feibel, C. S., Lepre, C. J., Prat, S., Lenoble, A., . . . Taylor, N. (2015). 3.3-Million-year-old stone tools from Lomekwi 3, West Turkana, Kenya. *Nature*, *521*, 310–315.

Helgason, B., Perilli, E., Schileo, E., Taddei, F., Brynjolfsson, S., & Viceconti, M. (2008). Mathematical relationships between bone density and mechanical properties: A literature review. *Clinical Biomechanics (Bristol, Avon)*, *23*, 135–146.

Hopkins, W. D. (1995). Hand preferences for a coordinated bimanual task in 110 chimpanzees (Pan troglodytes): Cross-sectional analysis. *Journal of Comparative Psychology*, *109*, 291–297.

Hopkins, W. D. (2008). Brief communication: Locomotor limb preferences in captive chimpanzees (Pan troglodytes): Implications for morphological asymmetries in limb bones. *American Journal of Physical Anthropology*, *137*, 113–118.

Hopkins, W. D. (2013). Neuroanatomical asymmetries and handedness in chimpanzees (Pan troglodytes): A case for continuity in the evolution of hemispheric specialization. *Annals of the New York Academy of Sciences*, *1288*, 17–35.

Hopkins, W. D., Phillips, K. A., Bania, A., Calcutt, S. E., Gardner, M., Russell, J., . . . Schapiro, S. J. (2011). Hand preferences for coordinated bimanual actions in 777 great apes: Implications for the evolution of handedness in hominins. *Journal of Human Evolution*, *60*, 605–611.

Hopkins, W. D., Reamer, L., Mareno, M. C., & Schapiro, S. J. (2015). Genetic basis in motor skill and hand preference for tool use in chimpanzees (Pan troglodytes). *Proceedings of the Royal Society B: Biological Sciences*, *282*, 20141223. AQ5

Hu, D., Ren, L., Howard, D., & Zong, C. (2014). Biomechanical analysis of force distribution in human finger extensor mechanisms. *BioMed Research International*, *2014*, 743460.

Hunt, K. D. (1991). Mechanical implications of chimpanzee positional behavior. *American Journal of Physical Anthropology*, *86*, 521–536.

Hunt, K. D. (1994). The evolution of human bipedality: Ecology and functional morphology. *Journal of Human Evolution*, *26*, 183–202.

Indersmitten, T., & Gur, R. C. (2003). Emotion processing in chimeric faces: Hemispheric asymmetries in expression and recognition of emotions. *The Journal of Neuroscience*, *23*, 3820–3825.

Judex, S., & Carlson, K. J. (2009). Is bone's response to mechanical signals dominated by gravitational loading? *Medicine and Science in Sports and Exercise*, *41*, 2037–2043.

Kanchan, T., Mohan Kumar, T. S., Pradeep Kumar, G., & Yoganarasimha, K. (2008). Skeletal asymmetry. *Journal of Forensic and Legal Medicine*, *15*, 177–179.

Kargov, A., Pylatiuk, C., Martin, J., Schulz, S., & Doderlein, L. (2004). A comparison of the grip force distribution in natural hands and in prosthetic hands. *Disability and Rehabilitation*, *26*, 705–711.

Keaveny, T. M., Morgan, E. F., Niebur, G. L., & Yeh, O. C. (2001). Biomechanics of trabecular bone. *Annual Review of Biomedical Engineering*, *3*, 307–333.

Key, A. J., & Dunmore, C. J. (2015). The evolution of the hominin thumb and the influence exerted by the non-dominant hand during stone tool production. *Journal of Human Evolution*, *78*, 60–69.

Key, A. J., & Lycett, S. J. (2011). Technology based evolution? A biometric test of the effects of hand size versus tool form on efficiency in an experimental cutting task. *Journal of Archaeological Science*, *38*, 1663–1670.

Ladd, A. L., Crisco, J. J., Hagert, E., Rose, J., & Weiss, A. P. (2014). The 2014 ABJS Nicolas Andry Award: The puzzle of the thumb: Mobility, stability, and demands in opposition. *Clinical Orthopaedics and Related Research*, *472*, 3605–3622.

Lambers, F. M., Bouman, A. R., Rimnac, C. M., & Hernandez, C. J. (2013). Microdamage caused by fatigue loading in human cancellous bone: Relationship to reductions in bone biomechanical performance. *PLoS One*, *8*, e83662.

Lambers, F. M., Koch, K., Kuhn, G., Ruffoni, D., Weigt, C., Schulte, F. A., & Müller, R. (2013). Trabecular bone adapts to long-term cyclic loading by increasing stiffness and normalization of dynamic morphometric rates. *Bone*, *55*, 325–334.

Landsmeer, J. M. (1955). Anatomical and functional investigations on the articulation of the human fingers. *Acta Anatomica Supplementum*, *25*, 1–69.

Lazenby, R. A. (1998). Second metacarpal cross-sectional geometry: Rehabilitating a circular argument. *American Journal of Human Biology*, *10*, 747–756.

Lazenby, R. A. (2002). Skeletal biology, functional asymmetry and the origins of "handedness". *Journal of Theoretical Biology*, *218*, 129–138.

Lazenby, R. A., Angus, S., Cooper, D. M., & Hallgrimsson, B. (2008). A three-dimensional microcomputed tomographic study of site-specific variation in trabecular microarchitecture in the human second metacarpal. *Journal of Anatomy*, *213*, 698–705.

Lazenby, R. A., Cooper, D. M., Angus, S., & Hallgrimsson, B. (2008). Articular constraint, handedness, and directional asymmetry in the human second metacarpal. *Journal of Human Evolution*, *54*, 875–885.

Lazenby, R. A., Skinner, M. M., Hublin, J. J., & Boesch, C. (2011). Metacarpal trabecular architecture variation in the chimpanzee (Pan troglodytes): Evidence for locomotion and tool-use? *American Journal of Physical Anthropology*, *144*, 215–225.

Lee, A. T., Williams, A. A., Lee, J., Cheng, R., Lindsey, D. P., & Ladd, A. L. (2013). Trapezium trabecular morphology in carpometacarpal arthritis. *Journal of Hand Surgery (American Volume)*, *38*, 309–315.

Lewis, J. W., Phinney, R. E., Brefczynski-Lewis, J. A., & DeYoe, E. A. (2006). Lefties get it "right" when hearing tool sounds. *Journal of Cognitive Neuroscience*, *18*, 1314–1330.

Li, Z. M., & Tang, J. (2007). Coordination of thumb joints during opposition. *Journal of Biomechanics*, *40*, 502–510.

Lieberman, D. E. (1996). How and why humans grow thin skulls: Experimental evidence for systemic cortical robusticity. *American Journal of Physical Anthropology*, *101*, 217–236.

Lieberman, D. E., Devlin, M. J., & Pearson, O. M. (2001). Articular area responses to mechanical loading: Effects of exercise, age, and skeletal location. *American Journal of Physical Anthropology*, *116*, 266–277.

Lozano, M., Mosquera, M., Bermúdez de Castro, J. M., Arsuaga, J. L., & Carbonell, E. (2009). Right handedness of Homo heidelbergensis from Sima de los Huesos (Atapuerca, Spain) 500,000 years ago. *Evolution and Human Behavior*, *30*, 369–376.

Macintosh, A. A., Pinhasi, R., & Stock, J. T. (2014). Divergence in male and female manipulative behaviors with the intensification of metallurgy in Central Europe. *PLoS One*, *9*, e112116.

Maga, M., Kappelman, J., Ryan, T. M., & Ketcham, R. A. (2006). Preliminary observations on the calcaneal trabecular microarchitecture of extant large-bodied hominoids. *American Journal of Physical Anthropology*, *129*, 410–417.

Maki, J., & Trinkaus, E. (2011). Opponens pollicis mechanical effectiveness in Neanderthals and early modern humans. *PaleoAnthropology*, *2011*, 62–71.

Maquer, G., Musy, S. N., Wandel, J., Gross, T., & Zysset, P. K. (2015). Bone volume fraction and fabric anisotropy are better determinants of trabecular bone stiffness than other morphological variables. *Journal of Bone and Mineral Research*, *30*, 1000–1008.

Marangoni, A., Belli, L. M., Caramelli, D., Jacopo, M.-C., Zavattaro, M., & Manzi, G. (2011). The Tierra del Fuego, its ancient inhabitants, and the collections of human skeletal remains in the Museums of Anthropology of Florence and Rome. Museological significance, past researches, perspectives. *Museologia Scientifica*, *5*, 88–96.

Marchant, L. F., & McGrew, W. C. (2007). Ant fishing by wild chimpanzees is not lateralised. *Primates*, *48*, 22–26.

Marchant, L. F., & McGrew, W. C. (2013). Handedness is more than laterality: Lessons from chimpanzees. *Annals of the New York Academy of Sciences*, *1288*, 1–8.

Marchi, D. (2005). The cross-sectional geometry of the hand and foot bones of the hominoidea and its relationship to locomotor behavior. *Journal of Human Evolution*, *49*, 743–761.

Marzke, M. W. (1997). Precision grips, hand morphology, and tools. *American Journal of Physical Anthropology*, *102*, 91–110.

Marzke, M. W. (2013). Tool making, hand morphology and fossil hominins. *Philosophical Transactions of the Royal Society of London Series B, Biological Sciences*, *368*, 20120414.

Marzke, M. W., Marchant, L. F., McGrew, W. C., & Reece, S. P. (2015). Grips and hand movements of chimpanzees during feeding in Mahale Mountains National Park, Tanzania. *American Journal of Physical Anthropology*, *156*, 317–326.

Marzke, M. W., Marzke, R. F., Linscheid, R. L., Smutz, P., Steinberg, B., Reece, S., & An, K. N. (1999). Chimpanzee thumb muscle cross sections, moment arms and potential torques, and comparisons with humans. *American Journal of Physical Anthropology*, *110*, 163–178.

Marzke, M. W., Toth, N., Schick, K., Reece, S., Steinberg, B., Hunt, K., . . . An, K. N. (1998). EMG study of hand muscle recruitment during hard hammer percussion manufacture of Oldowan tools. *American Journal of Physical Anthropology*, *105*, 315–332.

Marzke, M. W., & Wullstein, K. L. (1996). Chimpanzee and human grips: A new classification with a focus on evolutionary morphology. *International Journal of Primatology*, *17*, 117–139.

Matarazzo, S. (2013). Manual pressure distribution patterns of knuckle-walking apes. *American Journal of Physical Anthropology*, *152*, 44–50.

Mays, S. A. (2002). Asymmetry in metacarpal cortical bone in a collection of British post-mediaeval human skeletons. *Journal of Archaeological Science*, *29*, 435–441.

McGrew, W. C., & Marchant, L. F. (1992). Chimpanzees, tools, and termites: Hand preference or handedness? *Current Anthropology*, *33*, 114–119.

McGrew, W. C., & Marchant, L. F. (1997). On the other hand: Current issues in and meta-analysis of the behavioral laterality of hand function in nonhuman primates. *Yearbook of Physical Anthropology*, *40*, 201–232.

McManus, I. C., Davison, A., & Armour, J. A. (2013). Multilocus genetic models of handedness closely resemble single-locus models in explaining family data and are compatible with genome-wide association studies. *Annals of the New York Academy of Sciences*, *1288*, 48–58.

Meguerditchian, A., Vauclair, J., & Hopkins, W. D. (2010). Captive chimpanzees use their right hand to communicate with each other: Implications for the origin of the cerebral substrate for language. *Cortex*, *46*, 40–48.

Miller, C. T., & Paciulli, L. M. (2002). Patterns of lateralized hand use in an arboreal primate, *Simias concolor*. *American Journal of Primatology*, *56*, 231–236.

Mittra, E., Rubin, C., & Qin, Y. X. (2005). Interrelationship of trabecular mechanical and microstructural properties in sheep trabecular bone. *Journal of Biomechanics*, *38*, 1229–1237.

Morcillo, A., Fernandez-Carriba, S., & Loeches, A. (2006). Asymmetries in postural control and locomotion in chimpanzees (Pan troglodytes). *American Journal of Primatology*, *68*, 802–811.

Morgan, E. F., Bayraktar, H. H., & Keaveny, T. M. (2003). Trabecular bone modulus-density relationships depend on anatomic site. *Journal of Biomechanics*, *36*, 897–904.

Napier, J. R. (1960). Studies of the hands of living primates. *Proceedings of the Zoological Society of London*, *134*, 647–657.

Niewoehner, W. A. (2001). Behavioral inferences from the Skhul/Qafzeh early modern human hand remains. *Proceedings of the National Academy of Sciences of the United States of America*, *98*, 2979–2984.

Niewoehner, W. A. (2006). Neanderthal hands in their proper perspective. In K. Harvati & T. Harrison (Eds.), *Neanderthals revisited: New approaches and perspectives* (pp. 157–190). Dordrecht: Springer.

Niewoehner, W. A., Weaver, A. H., & Trinkaus, E. (1997). Neanderthal capitate-metacarpal articular morphology. *American Journal of Physical Anthropology*, *103*, 219–233.

Nikander, R., Sievanen, H., Heinonen, A., Daly, R. M., Uusi-Rasi, K., & Kannus, P. (2010). Targeted exercise against osteoporosis: A systematic review and meta-analysis for optimising bone strength throughout life. *BMC Medicine*, *8*, 47.

Nufer, P., Goldhahn, J., Kohler, T., Kuhn, V., Müller, R., & Herren, D. B. (2008). Microstructural adaptation in trapezial bone due to subluxation of the thumb. *Journal of Orthopaedic*, *26*, 208–216.

Odgaard, A. (1997). Three-dimensional methods for quantification of cancellous bone architecture. *Bone*, *20*, 315–328.

Olson, D., Ellis, J., & Nadler, R. (1990). Hand preference in captive gorillas, orang-utans and gibbons. *American Journal of Primatology*, *20*, 83–94.

Pahr, D. H., & Zysset, P. K. (2009). From high-resolution CT data to finite element models: Development of an integrated modular framework. *Computer Methods in Biomechanics and Biomedical Engineering*, *12*, 45–57.

Palmer, A. R. (1994). Fluctuating asymmetry analyses: A primer. In T. Markow (Ed.), *Developmental instability: Its origins and evolutionary implications* (pp. 335–364). Dordrecht, Netherlands: Springer.

Pataky, T. C., Slota, G. P., Latash, M. L., & Zatsiorsky, V. M. (2012). Radial force distribution changes associated with tangential force production in cylindrical grasping, and the importance of anatomical registration. *Journal of Biomechanics*, *45*, 218–224.

Paternoster, L., Lorentzon, M., Lehtimaki, T., Eriksson, J., Kahonen, M., Raitakari, O .... Mellström, D. (2013). Genetic determinants of trabecular and cortical volumetric bone mineral densities and bone microstructure. *PLoS Genetics*, *9*, e1003247.

Pearson, O. M., & Lieberman, D. E. (2004). The aging of Wolff's "law": Ontogeny and responses to mechanical loading in cortical bone. *American Journal of Physical Anthropology*, *39*, 63–99.

Phillipson, L. (1997). Eedge modifications as an indicator of function and handedness of Acheulian hand axes from Kariandusi, Kenya. *Lithic Technology*, *22*, 171–183.

Pontzer, H., Lieberman, D. E., Momin, E., Devlin, M. J., Polk, J. D., Hallgrimsson, B., & Cooper, D. M. (2006). Trabecular bone in the bird knee responds with high sensitivity to changes in load orientation. *The Journal of Experimental Biology*, *209*, 57–65.

Prowse, T. L., Saunders, S. R., Schwarcz, H. P., Garnsey, P., Macchiarelli, R., & Bondioli, L. (2008). Isotopic and dental evidence for infant and young child feeding practices in an imperial Roman skeletal sample. *American Journal of Physical Anthropology*, *137*, 294–308.

Rafferty, K. L., & Ruff, C. B. (1994). Articular structure and function in Hylobates, Colobus, and Papio. *American Journal of Physical Anthropology*, *94*, 395–408.

Rasband, W. S. (1997–2014). *Image J*. Bethesda, MD: U. S. National Institutes of Health.

Reznikov, N., Chase, H., Brumfeld, V., Shahar, R., & Weiner, S. (2015). The 3D structure of the collagen fibril network in human trabecular bone: Relation to trabecular organization. *Bone*, *71*, 189–195.

Robling, A. G. (2009). Is bone's response to mechanical signals dominated by muscle forces? *Medicine and Science in Sports and Exercise*, *41*, 2044–2049.

Rolian, C., Lieberman, D. E., & Zermeno, J. P. (2011). Hand biomechanics during simulated stone tool use. *Journal of Human Evolution*, *61*, 26–41.

Roth, H. L., Lora, A. N., & Heilman, K. M. (2002). Effects of monocular viewing and eye dominance on spatial attention. *Brain*, *125*, 2023–2035.

Roy, T. A., Ruff, C. B., & Plato, C. C. (1994). Hand dominance and bilateral asymmetry in the structure of the second metacarpal. *American Journal of Physical Anthropology*, *94*, 203–211.

Ruck, L., Broadfield, D. C., & Brown, C. T. (2015). Determining hominid handedness in lithic debitage: A review of current methodologies. *Lithic Technology*, *40*, 171–188.

Ruff, C. B., & Jones, H. H. (1981). Bilateral asymmetry in cortical bone of the humerus and tibia-sex and age factors. *Human Biology*, *53*, 69–86.

Ruff, C., Holt, B., & Trinkaus, E. (2006). Who's afraid of the big bad Wolff?: "Wolff's law" and bone functional adaptation. *American Journal of Physical Anthropology*, *129*, 484–498.

Rugg, G., & Mullane, M. (2001). Inferring handedness from lithic evidence. *Laterality*, *6*, 247–259.

Ryan, T. M., & Ketcham, R. A. (2002a). Femoral head trabecular bone structure in two omomyid primates. *Journal of Human Evolution*, *43*, 241–263.

Ryan, T. M., & Ketcham, R. A. (2002b). The three-dimensional structure of trabecular bone in the femoral head of strepsirrhine primates. *Journal of Human Evolution*, *43*, 1–26.

Ryan, T. M., & Krovitz, G. E. (2006). Trabecular bone ontogeny in the human proximal femur. *Journal of Human Evolution*, *51*, 591–602.

Ryan, T. M., & Shaw, C. N. (2012). Unique suites of trabecular bone features characterize locomotor behavior in human and non-human anthropoid primates. *PLoS One*, *7*, e41037.

Ryan, T. M., & Shaw, C. N. (2013). Trabecular bone microstructure scales allometrically in the primate humerus and femur. *Proceedings of the Royal Society B: Biological Sciences*, *280*, 20130172.

Ryan, T. M., & Shaw, C. N. (2015). Gracility of the modern Homo sapiens skeleton is the result of decreased biomechanical loading. *Proceedings of the National Academy of Sciences of the United States of America*, *112*, 372–377.

Ryan, T. M., & van Rietbergen, B. (2005). Mechanical significance of femoral head trabecular bone structure in loris and galago evaluated using micromechanical finite element models. *American Journal of Physical Anthropology*, *126*, 82–96.

Ryan, T. M., & Walker, A. (2010). Trabecular bone structure in the humeral and femoral heads of anthropoid primates. *Anatomical Record*, *293*, 719–729.

Sample, S. J., Behan, M., Smith, L., Oldenhoff, W. E., Markel, M. D., Kalscheur, V. L., . . . Muir, P. (2008). Functional adaptation to loading of a single bone is neuronally regulated and involves multiple bones. *Journal of Bone and Mineral Research*, *23*, 1372–1381.

Sarringhaus, L. A., MacLatchy, L. M., & Mitani, J. C. (2014) Locomotor and postural development of wild chimpanzees. *Journal of Human Evolution*, *66*, 29–38.

Sarringhaus, L. A., Stock, J. T., Marchant, L. F., & McGrew, W. C. (2005). Bilateral asymmetry in the limb bones of the chimpanzee (Pan troglodytes). *American Journal of Physical Anthropology*, *128*, 840–845.

Scher, f. H., & Tilgner, R. (2009). A new high-resolution computed tomography (CT) segmentation method for trabecular bone architectural analysis. *American Journal of Physical Anthropology*, *140*, 39–51.

Schipilow, J. D., Macdonald, H. M., Liphardt, A. M., Kan, M., & Boyd, S. K. (2013). Bone micro-architecture, estimated bone strength, and the muscle-bone interaction in elite athletes: An HR-pQCT study. *Bone*, *56*, 281–289.

Schulte, F. A., Ruffoni, D., Lambers, F. M., Christen, D., Webster, D. J., Kuhn, G., & Müller, R. (2013). Local mechanical stimuli regulate bone formation and resorption in mice at the tissue level. *PLoS One*, *8*, e62172.

Semaw, S., Rogers, M. J., Quade, J., Renne, P. R., Butler, R. F., Dominguez-Rodrigo, M., . . . Simpson, S. W. (2003). 2.6-Million-year-old stone tools and associated bones from OGS-6 and OGS-7, Gona, Afar, Ethiopia. *Journal of Human Evolution*, *45*, 169–177.

Shaw, C. N. (2011). Is 'hand preference' coded in the hominin skeleton? An *in-vivo* study of bilateral morphological variation. *Journal of Human Evolution*, *61*, 480–487.

Shaw, C. N., Hofmann, C. L., Petraglia, M. D., Stock, J. T., & Gottschall, J. S. (2012). Neanderthal humeri may reflect adaptation to scraping tasks, but not spear thrusting. *PLoS One*, *7*, e40349.

Shrewsbury, M. M., Marzke, M. W., Linscheid, R. L., & Reece, S. P. (2003). Comparative morphology of the pollical distal phalanx. *American Journal of Physical Anthropology*, *121*, 30–47.

Singh, I. (1979). Torsion in metacarpal bones and bilateral asymmetry. *Journal of Anatomy*, *129*, 343–349.

Skinner, M. M., Stephens, N. B., Tsegai, Z. J., Foote, A. C., Nguyen, N. H., Gross, T., . . . Kivell, T. L. (2015). Human-like hand use in *Australopithecus africanus*. *Science*, *347*, 395–399.

Smith, S. L. (2000). Shape variation of the human pollical distal phalanx and metacarpal. *American Journal of Physical Anthropology*, *113*, 329–348.

Stauber, M., Rapillard, L., van Lenthe, G. H., Zysset, P., & Müller, R. (2006). Importance of individual rods and plates in the assessment of bone quality and their contribution to bone stiffness. *Journal of Bone and Mineral Research*, *21*, 586–595.

Steele, J. (2004). When did directional asymmetry enter the record? In T. J. Crow (Ed.), *The speciation of modern Homo sapiens* (pp. 153–168). New York, NY: Oxford University Press.

Steele, J., & Uomini, N. (2005). Humans, tools and handedness. In V. Roux & B. Bril (Eds.), *Stone knapping: The necessary conditions for a uniquely hominid behaviour* (pp. 217–239). Cambridge: McDonald Institute for Archaeological Research.

Stock, J., & Pfeiffer, S. (2001). Linking structural variability in long bone diaphyses to habitual behaviors: Foragers from the southern African

Later Stone Age and the Andaman Islands. *American Journal of Physical Anthropology*, *115*, 337–348.

Stock, J. T. (2006). Hunter-gatherer postcranial robusticity relative to patterns of mobility, climatic adaptation, and selection for tissue economy. *American Journal of Physical Anthropology*, *131*, 194–204.

Stock, J. T., Shirley, M. K., Sarringhaus, L. A., Davies, T. G., & Shaw, C. N. (2013). Skeletal evidence for variable patterns of handedness in chimpanzees, human hunter-gatherers, and recent British populations. *Annals of the New York Academy of Sciences*, *1288*, 86–99.

Stout, D., & Chaminade, T. (2012). Stone tools, language and the brain in human evolution. *Philosophical Transactions of the Royal Society of London Series B, Biological Sciences*, *367*, 75–87.

Stout, D., Toth, N., Schick, K., & Chaminade, T. (2008). Neural correlates of Early Stone Age toolmaking: Technology, language and cognition in human evolution. *Philosophical Transactions of the Royal Society of London Series B, Biological Sciences*, *363*, 1939–1949.

Su, A., Wallace, I. J., & Nakatsukasa, M. (2013). Trabecular bone anisotropy and orientation in an early Pleistocene hominin talus from East Turkana, Kenya. *Journal of Human Evolution*, *64*, 667–677.

Sugiyama, T., Price, J. S., & Lanyon, L. E. (2010). Functional adaptation to mechanical loading in both cortical and cancellous bone is controlled locally and is confined to the loaded bones. *Bone*, *46*, 314–321.

Susman, R. L. (1979). Comparative and functional morphology of hominoid fingers. *American Journal of Physical Anthropology*, *50*, 215–236.

Tabiowo, E., & Forrester, G. S. (2013). Structured bimanual actions and hand transfers reveal population-level right-handedness in captive gorillas. *Animal Behaviour*, *86*, 1049–1057.

Tate, A. J., Fischer, H., Leigh, A. E., & Kendrick, K. M. (2006). Behavioural and neurophysiological evidence for face identity and face emotion processing in animals. *Philosophical Transactions of the Royal Society of London Series B, Biological Sciences*, *361*, 2155–2172.

Tocheri, M. W., Marzke, M. W., Liu, D., Bae, M., Jones, G. P., Williams, R. C., & Razdan, A. (2003). Functional capabilities of modern and fossil hominid hands: Three-dimensional analysis of trapezia. *American Journal of Physical Anthropology*, *122*, 101–112.

Tocheri, M. W., Orr, C. M., Jacofsky, M. C., & Marzke, M. W. (2008). The evolutionary history of the hominin hand since the last common ancestor of Pan and Homo. *Journal of Anatomy*, *212*, 544–562.

Toth, N. (1985). Archaeological evidence for preferential right-handedness in the lower and middle Pleistocene, and its possible implications. *Journal of Human Evolution*, *14*, 607–614.

Trinkaus, E., Churchill, S. E., & Ruff, C. B. (1994). Postcranial robusticity in Homo. II: Humeral bilateral asymmetry and bone plasticity. *American Journal of Physical Anthropology*, *93*, 1–34.

Trinkaus, E., & Villemeur, I. (1991). Mechanical advantages of the Neanderthal thumb in flexion: A test of an hypothesis. *American Journal of Physical Anthropology*, *84*, 249–260.

Tsegai, Z. J., Kivell, T. L., Gross, T., Nguyen, N. H., Pahr, D. H., Smaers, J. B., & Skinner, M. M. (2013). Trabecular bone structure correlates with hand posture and use in hominoids. *PLoS One*, *8*, e78781.

Ubelaker, D. H., & Zarenko, K. M. (2012). Can handedness be determined from skeletal remains? A chronological review of the literature. *Journal of Forensic Sciences*, *57*, 1421–1426.

Uchiyama, T., Tanizawa, T., Muramatsu, H., Endo, N., Takahashi, H. E., & Hara, T. (1999). Three-dimensional microstructural analysis of human trabecular bone in relation to its mechanical properties. *Bone*, *25*, 487–491.

Uomini, N. T. (2009). The prehistory of handedness: Archaeological data and comparative ethology. *Journal of Human Evolution*, *57*, 411–419.

Uomini, N. T. (2011). Handedness in Neanderthals. In N. J. Conard & J. Richter (Eds.), *Neanderthal lifeways, subsistence and technology: One hundred fifty years of Neanderthal study* (pp. 139–154). New York, NY: Springer.

Van Valen, L. (1962). A study of fluctuating asymmetry. *Evolution*, *16*, 125–142.

Villemeur, I. (1994). *La main des Néandertaliens: Comparaison avec la main des hommes de type moderne, morphologie et mécanique*. Paris: Editions du CNRS.

Vlček, E. (1975). Morphology of the first metacarpal of Neanderthal individuals from the Crimea. *Bulletins et Mémoires de la Société d'Anthropologie de Paris*, *2*, 257–276.

Volpato, V., Macchiarelli, R., Guatelli-Steinberg, D., Fiore, I., Bondioli, L., & Frayer, D. W. (2012). Hand to mouth in a Neanderthal: Right-handedness in Regourdou 1. *PLoS One*, *7*, e43949.

Wallace, I. J., Judex, S., & Demes, B. (2015). Effects of load-bearing exercise on skeletal structure and mechanics differ between outbred populations of mice. *Bone*, *72*, 1–8.

Wallace, I. J., Middleton, K. M., Lublinsky, S., Kelly, S. A., Judex, S., Garland, T., Jr., & Demes, B. (2010). Functional significance of genetic variation underlying limb bone diaphyseal structure. *American Journal of Physical Anthropology*, *143*, 21–30.

Wallace, I. J., Pagnotti, G. M., Rubin-Sigler, J., Naeher, M., Copes, L. E., Judex, S., . . . Demes, B. (2015). Focal enhancement of the skeleton to exercise correlates with responsivity of bone marrow mesenchymal stem cells rather than peak external forces. *The Journal of Experimental Biology*, *218*, 3002–3009.

Weiss, D. J., Ghazanfar, A. A., Miller, C. T., & Hauser, M. D. (2002). Specialized processing of primate facial and vocal expressions: Evidence for cerebral asymmetries. In L. J. Rogers & R. J. Andrew (Eds.), *Comparative vertebrate lateralization* (pp. 480–530). Cambridge: Cambridge University Press.

Williams, E. M., Gordon, A. D., & Richmond, B. G. (2012). Hand pressure distribution during Oldowan stone tool production. *Journal of Human Evolution*, *62*, 520–532.

Wunderlich, R. E., & Jungers, W. L. (2009). Manual digital pressures during knuckle-walking in chimpanzees (Pan troglodytes). *American Journal of Physical Anthropology*, *139*, 394–403.

Yerges, L. M., Klei, L., Cauley, J. A., Roeder, K., Kammerer, C. M., Ensrud, K. E, . . . Moffett, S. P. (2010). Candidate gene analysis of femoral neck trabecular and cortical volumetric bone mineral density in older men. *Journal of Bone and Mineral Research*, *25*, 330–338.

Zysset, P. K. (2003). A review of morphology-elasticity relationships in human trabecular bone: Theories and experiments. *Journal of Biomechanics*, *36*, 1469–1485.

# AUTHOR QUERY FORM

Dear Author,
During the preparation of your manuscript for publication, the questions listed below have arisen. Please attend to these matters and return this form with your proof.
Many thanks for your assistance.

| Query References | Query | Remarks |
|---|---|---|
| AQ1 | Please check all the heading levels. | |
| AQ2 | Please check insertion of reference citation "Lazenby, Angus, Cooper, & Hallgrimsson (2008)." | |
| AQ3 | Please check the page range for reference "Almécija et al. (2015)." | |
| AQ4 | Please provide the last page number for references "Christen et al. (2014), Gross et al. (2014), and Nikander et al. (2010)." | |
| AQ5 | Please check and provide the page range for references "Hopkins et al. (2015), Hu et al. (2014), Marzke (2013), and Ryan and Shaw (2013)." | |
| AQ6 | Please provide the note for bold values in Tables 2 and 3, if applicable. | |
| AQ7 | Please provide complete details for Schilling et al. (2013), Shaw and Ryan (2012), Morgan et al. (2015), and Xhae et al., 2015 in the reference list or delete the citation from the text. | |
| AQ8 | There is no mention of Dempster and Raisz (2015) and Churchill (2001) in the text. Please insert a citation in the text or delete the reference as appropriate. | |
| AQ9 | Please confirm that given names (red) and surnames/family names (green) have been identified correctly. | |